Astrocyte beta-adrenergic receptor activity regulates neuronal NMDA receptor signaling

A DISSERTATION

SUBMITTED TO THE FACULTY OF

THE UNIVERSITY OF MINNESOTA

BY

Armani P. Del Franco

ADVISOR: Eric A. Newman

June 2023

Acknowledgements

I thank my thesis advisor, Eric Newman, for his unwavering support and helping me become a better scientist. You allowed me to ask questions and develop this thesis project, which was so empowering. But you also kept me focused and helped me see my ideas through. Thank you for all your patience and feedback with my writing and presenting, and providing an opportunity to TA for you, you've helped me improve so much as a communicator as well. The enthusiasm you bring to any topic and project are elements I hope to bring to any project I pursue in the future.

I thank everyone in lab who created a supportive environment, as mentors, colleagues and friends. Thank you so much to Pei-Pei Chiang for performing surgeries, genotyping and keeping the lab running smoothly. Your kindness helped me get through.

Amy Nippert, thank you for showing me the ropes in lab and teaching me to do in vivo imaging. Your friendship, companionship and snacks inside and out of lab created such an engaging environment full of laughs and ponderings.

Chloe Cable, thank you for being my lab twin and always being there to support me through struggle and triumph. Your support, editing and bouncing ideas around, and company continue to brighten my days.

Thank you, Sid Kuo, for showing me how to use the 2-photon and confocal, teaching me how to perform electrophysiology and being available any time for whatever questions I may have had. Your knowledge and precision have made me a better scientist; this thesis would have never happened without you.

I thank my thesis committee, Alfonso Araque, Stan Thayer, and Julia Lemos for their feedback and advice throughout the design and refinement of my experiments.

I thank Alfonso, Stan, and Paulo Kofuji for lending equipment and aid that were invaluable in carrying out my experiments.

I thank the GPN for its supportive community and especially my class of 2017 who helped make Minnesota feel like home during my PhD.

Finally, thank you to my family for always encouraging me to pursue my passions and dreams. Thank you for instilling me with a curious mind and for listening no matter what.

Abstract

Glutamate spillover from the synapse is tightly regulated by astrocytes, limiting the activation of extrasynaptically located NMDA receptors (NMDAR). The processes of astrocytes are dynamic and can affect synaptic physiology. Though norepinephrine (NE) and β-adrenergic receptor (β-AR) activity can modify astrocyte volume, this has yet to be confirmed outside of sensory cortical areas, nor has the effect of noradrenergic signaling on glutamate spillover and neuronal NMDAR activity been explored.

We monitored changes to astrocyte process volume in response to noradrenergic agonists in the medial prefrontal cortex of male and female mice. Both NE and the β-AR agonist isoproterenol (ISO) increased process volume by 18%, significantly higher than changes seen in aCSF or when astrocytes had G-protein signaling blocked by GDPβS. We then measured the effect of β-AR signaling on evoked NMDAR currents. While ISO did not affect single stimulus excitatory currents of Layer 5 pyramidal neurons, ISO reduced NMDAR currents evoked by 10 stimuli at 50 Hz, which elicits glutamate spillover, by 18%.

After isolating extrasynaptic NMDARs by blocking synaptic NMDARs with the activity-dependent NMDAR blocker MK-801, ISO similarly reduced extrasynaptic NMDAR currents in response to 10 stimuli by 16%. Finally, blocking β-AR signaling in the astrocyte network, by loading them with GDPβS, reversed the ISO effect on 10 stimuli-evoked NMDAR currents. These results demonstrate that astrocyte β-AR activity reduces glutamate spillover and extrasynaptic NMDAR recruitment.

Table of contents

List of Figures

Chapter 1: Introduction

Overview

Astrocytes play an essential role in the proper functioning of the nervous system, including regulation of glutamate signaling (Walz and Mukerji, 1988; Araque et al., 1999a; Newman, 2002; Bay and Butt, 2012; Fernandez et al., 2022). Peripheral astrocyte processes (PAPs) are closely associated with synapses, and act as the primary source of glutamate uptake and barriers to diffusion, limiting glutamate spillover (Rusakov, 2001; Huang and Bordey, 2004; Takayasu et al., 2006; Hires et al., 2008). However, glutamate spillover does occur, activating extrasynaptically located NMDA receptors (NMDAR) (Chen and Diamond, 2002; Nie and Weng, 2009; Chalifoux and Carter, 2011; Henneberger et al., 2020). Spillover can have varied physiological consequences, including heterosynaptic depression and excitotoxicity (Zhang and Sulzer, 2003; Hardingham and Bading, 2010; Henneberger et al., 2020).

Astrocyte morphology is dynamic and changes to PAP volume and their proximity to synapses influence glutamate signaling (Oliet et al., 2004; Henneberger et al., 2020; Müller et al., 2021). Several molecules and physiological conditions have been found to influence astrocyte morphology, including norepinephrine (NE) (Xie et al., 2013; Vardjan et al., 2014; Sherpa et al., 2016). Through the activation of β adrenergic receptors (β-AR), norepinephrine causes PAP expansion, increasing astrocyte process volume (Sherpa et al., 2016).

However, these observations have only been made in sensory cortical regions or in culture. Other brain regions where NE signaling is of vital importance, like the emotion processing medial prefrontal cortex (mPFC) (Santana and Artigas, 2017), have gone unexplored. Similarly, the influence of NE and β-AR signaling on glutamate spillover

remains unanswered, especially with regards to what role astrocytes play in mediating those changes. This thesis tests three main hypotheses.

1) Noradrenergic activity via NE and β-AR signaling increase astrocyte process volume in the mPFC.

2) β-AR signaling reduces NMDAR activity, including extrasynaptic NMDARs.

3) Changes to NMDAR activity are due to astrocyte β-AR signaling.

Astrocyte physiology and role at the synapse

Until recently, astrocytes and other glia were considered an afterthought in the brain, relegated to being the glue that held neurons in place (Somjen, 1988). However, the previous 40+ years of research have ushered in a new understanding of how vital astrocytes are to the nervous system, both as a homeostatic regulator of multiple pathways (Huang et al., 1993; Jung et al., 1994; Hertz and Chen, 2016) and through active communication with neurons (D'Ascenzo et al., 2007; Halassa et al., 2007a) and other glia (Kettenmann and Ransom, 1988; Schipke et al., 2002). Astrocytes are responsible for maintaining ion homeostasis (Newman et al., 1984; Newman, 1999; Hertz and Chen, 2016) and neurotransmitter uptake (Albrecht et al., 1985; Wilson and Walz, 1988; Amundson et al., 1992; Rose et al., 2018), providing metabolic support (Walz and Mukerji, 1988; Nortley and Attwell, 2017), release gliotransmitters to modulate neuronal circuit activity (D'Ascenzo et al., 2007; Martineau et al., 2008; Covelo and Araque, 2018), contribute to synaptogenesis (Kucukdereli et al., 2011; Tsai et al., 2012; Stogsdill et al., 2017) and synaptic plasticity (Navarrete et al., 2012; Valtcheva and Venance, 2016; Hösli et al., 2022), and play a role in neurovascular coupling through specialized processes called endfeet (Dunn et al., 2013; Biesecker et al., 2016; Mishra

et al., 2016). Protoplasmic astrocytes that reside in the grey matter of the brain form non-overlapping territories that tile the nervous system and carry out these various functions through their uniquely complex, bush-like morphology (Bushong et al., 2002; Halassa et al., 2007b; Minge et al., 2021). It has been estimated that a single mouse astrocyte contacts 10,000s of synapses with their fine peripheral astrocyte processes (PAPs), through which astrocytes monitor and respond to local activity (Bushong et al., 2002; Oberheim et al., 2006; Halassa et al., 2007b). Astrocytes have been shown to respond to local glutamatergic (Cornell-Bell et al., 1990; De Pittà et al., 2009; Stobart et al., 2018; Arizono et al., 2020) and GABAergic signaling (MacVicar et al., 1989; Israel et al., 2003), volume signaling by monoaminergic neuromodulators (Duffy and Macvicar, 1995; Bekar et al., 2008; Corkrum et al., 2020) and neuro-hormones (Theodosis and Poulain, 2001; Li et al., 2006), lipids (Bezzi et al., 1998; Manning et al., 1998), inflammatory molecules (Bezzi et al., 2001; Habbas et al., 2015) and the extracellular matrix (Johnson et al., 2015). Through gap junctions, astrocytes form networks that coordinate populations of synapse and neuronal responses (Rose and Ransom, 1997; Houades et al., 2008).

Proper synaptic communication relies on the tight regulation of glutamate transmission and limited glutamate spillover (Huang and Bordey, 2004; Allam et al., 2012; Parsons et al., 2016). Glutamate is the primary excitatory signaling molecule that drives neuronal and network activity (Collingridge and Singer, 1990; Marvin et al., 2013). Glutamate receptor signaling, especially through the activation of coincident detecting and Ca^{2+} permeable NMDA receptors (NMDARs), is responsible for some models of glutamate-mediated synaptic plasticity (Collingridge and Singer, 1990; Bear, 1996; Wang et al., 2008). Proper maintenance and tuning of synaptic responses to glutamatergic

inputs, which coordinate neuronal excitation and behavior, rely upon the high signal fidelity found at glutamatergic synapses (Rusakov, 2001; Takayasu et al., 2006).

Astrocytes are the primary regulators of glutamate transmission (Rothstein et al., 1996; Bergles and Jahr, 1998; Allam et al., 2012). Their fine processes closely associate with synapses, acting as the primary means of glutamate uptake and barriers to limit glutamate diffusion out of the synapse (Rusakov, 2001; Heller et al., 2019). Primary expression of glutamate transporters (EAAT1 and EAAT2), are expressed by astrocytes and enriched in PAPs associated with glutamatergic synapses (Rauen et al., 1996; Harada et al., 1998; Genoud et al., 2006). Astrocyte processes help isolate individual synapses from each other, despite their proximity, and provide a threshold for the recruitment of additional receptors and synapses (Huang and Bordey, 2004; Nie and Weng, 2009). Extrasynaptic receptor recruitment can be achieved through strong enough stimulation and overwhelming regulatory mechanisms, or through changes to astrocyte regulation of glutamate signaling (Harris and Pettit, 2008; Chalifoux and Carter, 2011; Henneberger et al., 2020). Therefore, it is possible for glutamate to escape the synaptic compartment and result in glutamate spillover, activating extrasynaptically expressed receptors or resulting in synaptic crosstalk.

Extrasynaptic NMDA receptors signaling and consequences of glutamate spillover

Synaptic and extrasynaptic NMDA receptors

Glutamate spillover from the synapse recruits differentially expressed receptors at the extrasynaptic regions of a synapse, receptors that are expressed outside of the postsynaptic density (Baude et al., 1993; Scimemi et al., 2004; Delgado et al., 2018). Multiple different metabotropic glutamate receptors are enriched in the extrasynaptic

region, as well as NMDARs (D'Ascenzo et al., 2007; Harris and Pettit, 2008; Anderson et al., 2015; Scheefhals et al., 2023). Extrasynaptic NMDARs are largely comprised of different subunits compared to synaptic NMDARs, each displaying different Ca^{2+} permeabilities and receptor kinetics (Zhou et al., 2013; Delgado et al., 2018). Furthermore, studies show synaptic and extrasynaptic NMDARs interact with different intracellular machinery, resulting in different downstream consequences (Hardingham et al., 2002; Hardingham and Bading, 2010; Li et al., 2018).

While all NMDARs have two GluN1 subunits, there are various GluN2 subunits, with GluN2A and GluN2B being the most prevalent (Hardingham and Bading, 2010; Zhou et al., 2013). GluN2B-containing NMDARs are the primarily expressed NMDAR during adolescence, and get switched out for GluN2A-containing NMDARs during development (Wang et al., 2011; Dupuis et al., 2014). These GluN2A-containing NMDARs become enriched during adulthood, especially at the synapse, and are a marker for mature synapses (Flint et al., 1997). GluN2B-containing NMDARs seem to remain enriched extrasynaptically (Dupuis et al., 2014; Delgado et al., 2018; Veruki et al., 2019; Tang et al., 2020). The exclusive localized expression of GluN2B-containing NMDARs, however, remains debated, as some studies show GluN2A and GluN2B subunits are found to be expressed in extrasynaptic and synaptic regions, respectively (Pousinha et al., 2017; Chiu et al., 2019). Still, GluN2A-containing NMDARs are found primarily at the synapse and GluN2B-containing NMDARs are primarily at extrasynaptic sites after reaching adulthood. For example, studies recording NMDAR currents at synaptic vs extrasynaptic sites were able to primarily block extrasynaptic NMDAR currents with GluN2B-specific antagonists in rodent hippocampus and frontal cortical areas (Milnerwood et al., 2010; Papouin et al., 2012; Hanson et al., 2015; Yang et al.,

2017). These studies were able to isolate extrasynaptic NMDARs by blocking synaptic NMDARs with an activity-dependent blocker MK-801. Delivering several single electric stimuli that elicit the release of glutamate restricted to the synapse eventually block evoked synaptic NMDAR current (Harris and Pettit, 2008; Milnerwood et al., 2010; Yang et al., 2017). Extrasynaptic NMDAR currents were then recruited by delivering multiple stimuli at a rate faster than 10Hz (Harris and Pettit, 2008).

Synaptic and extrasynaptic NMDARs seem to rely more heavily on different co-agonists to bind the NMDAR in order to open. The NMDAR co-agonist site was first discovered to bind glycine and is aptly called the glycine binding site, but endogenous D-serine acts as another potent co-agonist (Henneberger et al., 2010; Klatte et al., 2013). While extrasynaptic NMDARs rely more upon glycine binding, synaptic NMDARs rely more upon D-serine (Papouin et al., 2012). Prior studies suggest different enriched GluN2 subunits have different binding affinities for glycine or D-serine (Mori and Mishina, 1995). Astrocyte process proximity not only influences glutamate spillover, it may also maintain co-agonist concentration gradients through determining the distribution of co-agonist targeting enzymes and diffusion of co-agonists themselves (Berger et al., 1998; Stevens et al., 2010). Both glycine and D-serine have been shown to be released by astrocytes, with various stimuli leading to their release (Henneberger et al., 2010; Shibasaki et al., 2017).

Consequences of extrasynaptic NMDA receptor activity

Extrasynaptic and synaptic NMDAR activity recruit different signaling pathways that result in different functional consequences. The localization of different intracellular proteins to the extrasynaptic or synaptic compartment and specific protein interactions

with the GluN2B or GluN2A C-terminus may contribute to which downstream signaling pathways get recruited. Generally, while synaptic NMDAR activity is associated with long term potentiation (LTP) and strengthening synapses, extrasynaptic activity is associated with long term depression (LTD) and removal of dendritic spines (Liu et al., 2013; Delgado et al., 2018). While synaptic NMDAR activity is associated with activating cell-survival molecules like ERK1/2, pCREB, and BDNF, extrasynaptic NMDAR activity is associated with increasing cell-death pathway activity by recruiting DAPK1, p38MAPK, FoxO3a, and Calpain (Hardingham et al., 2002; Ivanov et al., 2006; Kaufman et al., 2012; Zhou et al., 2013; Parsons and Raymond, 2014; Li et al., 2018). Extrasynaptic enriched GluN2B-containing NMDARs also seem to interact with several molecules associated with GluN2A-containing NMDARs in a bidirectional way, either physiologically or pathologically (Ivanov et al., 2006; Hardingham and Bading, 2010; Zhou et al., 2013). While potentially aiding in activating CREB under certain physiological conditions, pathological overactivation of extrasynaptic GluN2B-containing NMDARs can result in ERK1/2 and CREB inhibition (Hardingham et al., 2002; Kaufman et al., 2012).

Extrasynaptic NMDAR activity has been linked to negative health consequences of excitotoxicity, which is tied to GluN2B-containing NMDARs having a larger Ca^{2+} permeability and slower decay kinetics compared to other NMDARs. (Rothman and Olney, 1987; Zhou et al., 2013). Enhanced extrasynaptic NMDAR activity from extrasynaptic glutamate contributes to phenotypes found in animals models of chronic stress and epilepsy (Tanaka et al., 1997; Coulter and Eid, 2012; Miller et al., 2014; Li et al., 2018). In the case of chronic stress, elevated extracellular glutamate levels are observed, and uncoupling GluN2B-containing NMDAR activity's recruitment of DAPK1 has antidepressant effects (Li et al., 2018). Similarly, it is thought that the fast-acting

antidepressant effects of low dose NMDAR antagonists preferably bind to extrasynaptic NMDARs (Miller et al., 2014; Tang et al., 2020). Synaptic and extrasynaptic NMDAR activity are imbalanced in other neurological disorders. Enhanced extrasynaptic NMDAR currents are observed in mouse models of Huntington's disease (Milnerwood et al., 2010). Meanwhile, in mouse models of Alzheimer's disease extrasynaptic NMDAR contributions to overall NMDAR signaling increase, producing pathological outcomes for cells (Hanson et al., 2015; Pallas-Bazarra et al., 2019).

What factors contribute to glutamate spillover?

Regulation of glutamate spillover and balancing NMDAR activity help shape synaptic physiology and behavior. Limiting extrasynaptic NMDAR activity allows for its modulation by certain physiological triggers or pathology (Oliet et al., 2001; Takayasu et al., 2006; Nie and Weng, 2009; Henneberger et al., 2020). There are several factors that contribute to glutamate spillover, including changes to glutamate transport and ECS volume fraction.

Glutamate transporters

Glutamate spillover is affected by changes to astrocyte-mediated glutamate transport and their expression of EAAT1 and EAAT2 (Genoud et al., 2006). The pharmacological blockade of astrocyte glutamate transport with TBOA results in a slower termination of glutamate signaling and glutamate spreading beyond the synapse (Hires et al., 2008; Romanos et al., 2019; Herde et al., 2020). This elicits extrasynaptic NMDAR activation as well as other cells through synaptic crosstalk (Piet et al., 2004; Potapenko et al., 2013). Studies show that impaired glutamate transport can result in seizure-like

activity and induce excitotoxicity (Rothstein et al., 1996; Tanaka et al., 1997; Boison, 2012). Changes to glutamate transport expression have also been found in psychiatric disorders including addiction and major depression (McCullumsmith and Sanacora, 2015; Li et al., 2018). Impaired glutamate uptake coincides with higher tonic extracellular glutamate, contributing to extrasynaptic NMDAR activation and depressive-like behavior in chronically stressed mice (Li et al., 2018). Meanwhile, in rat addiction studies, withdrawal coincides with the downregulation of astrocyte glutamate transporters (McCullumsmith and Sanacora, 2015; Kim et al., 2018). Subsequent activity elicited by a drug-paired cue then overwhelms transporters, resulting in transient plasticity and triggering drug seeking behavior.

Extracellular space

Astrocyte processes help define the space glutamate can diffuse through (Rusakov, 2001; Witcher et al., 2010; Heller et al., 2019). Changes to astrocyte morphology not only affect the proximity of glutamate transporters to the synapse, it also influences ECS volume fraction (Oliet et al., 2001; Piet et al., 2004; Sherpa et al., 2016; Walch et al., 2020). Both ECS volume fraction and tortuosity, or how convoluted a path is for a molecule to diffuse through, influence how molecules move through space. Changes to the ECS lead to varied diffusion rates and affect glutamate spillover (Nicholson and Phillips, 1981; Kinney et al., 2013; Kuo et al., 2020). While smaller ECS volume fraction results in higher concentrations of neurotransmitter near a release site, the diffusion away is greatly limited, especially by the presence of nearby transporters. However, larger ECS volume fraction leads to a smaller concentration remaining at the point of release, and a greater concentration of neurotransmitter spreads to bind farther

away receptors (Sykova and Nicholson, 2008; Nicholson et al., 2011; Henneberger et al., 2020). ECS volume fraction can be measured using real time iontophoresis, by calculating the diffusion of tetramethylammonium (TMA^+) to an ion-sensitive electrode a fixed distance away (Nicholson and Phillips, 1981; Xie et al., 2013; Sherpa et al., 2016). Another method uses optical imaging to measure the diffusion of small fluorophores through space (Binder et al., 2004; Zhang and Verkman, 2010). Both techniques have been used in brain slice and in vivo to calculate the properties of diffusion through ECS.

Utilizing these techniques, studies have found ECS volume fraction to be dynamic and capable of changing under various conditions. ECS volume fraction varies by region, potentially contributing to signaling qualities of specific brain areas (Zhang and Verkman, 2010). Age also affects ECS volume fraction and is much larger in the young, developing brain and retina compared to adulthood (Lehmenkuhler et al., 1993; Larsen et al., 2019; Kuo et al., 2020). A larger ECS volume fraction in early development may contribute to certain synchronized activities and coordinated waves of activity observed in the brain and the retina during development. Even throughout the day, ECS volume fraction fluctuates between wakefulness and sleep states (Xie et al., 2013; Cooper et al., 2018). NE signaling contributes to ECS volume fraction being around 14% when NE tone is at its highest, during wakefulness, and being around 24% during sleep, when NE tone is at its lowest (Xie et al., 2013). Other neuromodulators, neuronal activity fluctuations, and $[K^+]_e$ levels associated with arousal may also contribute (Ding et al., 2016). Evoked neuronal activity has also been shown to reduce local ECS volume fraction, both in the brain and retina (Svoboda and Sykova, 1991; Haj-Yasein et al., 2012; Kuo et al., 2020). Some studies have also confirmed changes to ECS volume fraction affect glutamate spillover (Piet et al., 2004).

So far, changes to astrocyte volume have been found responsible for observed changes in ECS volume fraction. Astrocytes possess a unique morphology that is comprised of thousands of fine processes that have much more surface area compared to volume and are structures capable of driving large changes to ECS in the syncytium (Sherpa et al., 2016; Larsen and MacAulay, 2017; Henneberger et al., 2020; Walch et al., 2020; Minge et al., 2021). Changes to ECS volume fraction coincide with changes to astrocyte process synaptic coverage which also influence glutamate spillover.

Mechanisms for astrocyte morphological changes and consequences

Various mechanisms contribute to the astrocyte morphology and process volume changes observed in healthy, disrupted and pathological systems. The following examples highlight what circumstances elicit astrocyte morphological change and whether there were associated changes to neuronal signaling. Perturbing the brain through applying osmotic pressure or increasing $[K^+]_e$ affect astrocyte process volume (Walz, 1992; Kimelberg et al., 1995; Wurm et al., 2008). Creating an osmotic challenge by exposing slices to either higher or lower osmolarity artificial CSF (aCSF) causes processes to shrink or swell, respectively (Kimelberg et al., 1995; Song et al., 2015; Kuo et al., 2020). These changes in cell volume seem to occur primarily in astrocytes and drive changes to ECS volume fraction. Enriched expression of aquaporin 4 (AQP4), a water channel, may contribute to astrocyte sensitivity to changes in osmolarity (Haj-Yasein et al., 2012; Jo et al., 2015; Lisjak et al., 2017). However, various conditions that result in astrocyte swelling have been found to be AQP4 independent, suggesting there are other means for water to traverse astrocyte membranes (Larsen and MacAulay, 2017; Walch et al., 2020; Colbourn et al., 2021).

Astrocytes are a primary regulator of $[K^+]_e$ levels. Through the enriched expression of various K^+ channels or transporters like Kir4.1 and Na^+K^+-ATPase, (Neusch et al., 2006; Bay and Butt, 2012; Larsen et al., 2014; Walch et al., 2020) astrocytes help return high $[K^+]_e$ back to resting $[K^+]_e$ levels after periods of high neuronal activity. (Kucheryavykh et al., 2007; Chever et al., 2010; Bay and Butt, 2012). These periods of high neuronal activity elicit increases in astrocyte process volume (Walz, 1987; Kimelberg et al., 1995; Walch et al., 2020; Toft-Bertelsen et al., 2021). In both the brain and the retina, studies found that bicarbonate ion flux contributes to the observed swelling of glial processes (Florence et al., 2012; Chiang et al., 2022). Meanwhile, other work found Na^+K^+-ATPase activity was responsible for process swelling caused by artificially increasing $[K^+]_e$ or changing osmolality (Larsen et al., 2014; Song et al., 2015; Walch et al., 2020).

Oxytocin, a hormone and neuroendocrine molecule important in reproductive systems and social behavior, also modifies astrocyte morphology (Theodosis and Poulain, 2001). In the hypothalamic supraoptic (SON) and paraventricular nucleus (PVN) of lactating rats, elevated oxytocin levels cause astrocyte processes to retract (Oliet et al., 2004; Piet et al., 2004). This results in glutamate spillover from evoked glutamatergic inputs, activating presynaptic mGluR3 on GABAergic inputs, and led to the heterosynaptic depression of GABAergic inputs and enhanced circuit excitability (Piet et al., 2004).

LTP is a critical process that strengthens synaptic units and influences astrocyte morphology in the hippocampus (Perez-Alvarez et al., 2014; Henneberger et al., 2020; Herde et al., 2020). By dye-filling astrocytes and comparing the relative fluorescence intensity of filled processes to the intensity of the soma (100% volume), researchers

measured absolute astrocyte process volume and how it changed (Henneberger et al., 2020; Minge et al., 2021). The repeated, high-intensity stimuli needed to elicit LTP induction and the repeated presentation of uncaged glutamate at a synapse caused corresponding astrocyte processes to retract. Not only did individual processes appear to retract, high-frequency stimulation reduced overall astrocyte process volume (Henneberger et al., 2020). Reducing astrocyte process volume increased glutamate travel distance and widened extracellular glutamate diffusion based on recordings using glutamate sensors. In line with astrocyte process retraction producing glutamate spillover, synaptic crosstalk was also observed. High-frequency stimulation activated astrocytic NKCC1 and cofilin, which led to process remodeling (Henneberger et al., 2020). However, conflicting studies reported LTP induction resulted in closer association of fluorescing astrocyte processes to hippocampus neuron spines (Perez-Alvarez et al., 2014). These reports did not measure global process volume changes and used stimulus protocols to elicit LTP through spike-timing dependent plasticity (STDP). Perhaps different LTP induction methods promote different types of activity in astrocytes, or there is a bidirectional regulation of astrocyte process proximity to specific subclasses of synapses, related to spine or synapse type.

Caloric restriction has been shown to improve cognitive performance and memory (Sohal and Weindruch, 1996; Acosta-Rodríguez et al., 2022). Researchers found caloric restriction affects astrocyte morphology (Popov et al., 2020). Compared to mice on standard diets, hippocampal astrocyte process volume was larger in caloric restricted mice. Increased astrocyte volume coincided with more effective K^+ clearance and glutamate uptake, and reduced extrasynaptic GluN2B NMDAR activation (Popov et al., 2020). However, pathways responsible for increasing astrocyte volume are unknown.

Recent work has centered around the ability of RhoA signaling to affect astrocyte morphology through stabilizing actin (Renault-Mihara et al., 2017; Müller et al., 2021; Domingos et al., 2023). Astrocytes express several types of receptors that elicit RhoA signaling including serotonin, a monoamine critical in emotion processing, learning and memory (Walz, 1988; Wotton et al., 2020). Specifically, serotonin receptor 4 (5-HT_4R) expressed by hippocampal astrocytes. 5-HT_4R is a $G\alpha_{13}$ G-protein coupled receptor (GPCR) that elicits increases to RhoA signaling. As such, 5-HT_4R agonist BIMU8 induced astrocyte process retractions (Müller et al., 2021). Likewise, the direct manipulation of RhoA activity by virally expressing a constitutively active RhoA reduced astrocyte process volume (Domingos et al., 2023).

As previously mentioned, ECS volume fraction varies between wakefulness (14%) and sleep (24%) (Xie et al., 2013). NE signaling is highest during wakefulness and reduces ECS volume fraction. Eliminating NE signaling caused wakefulness ECS volume fraction to become like those during sleep (Xie et al., 2013). So far, studies looking ECS volume fraction during wakefulness and sleep have not directly investigated astrocyte volume changes. However, prior work in culture had found that β-adrenergic receptor (β-AR) activity resulted in morphological changes, increasing stellation and complexity of processes (Vardjan et al., 2014). In rat visual cortex, β-AR agonist incubation shrank ECS volume fraction by 30% (Sherpa et al., 2016). Coinciding with these measures, electron microscopy revealed that β-AR activity increased astrocyte process membrane and cytoplasm volume, increasing astrocyte process volume. This suggests that astrocyte β-ARs reduce ECS volume fraction and contribute to the smaller ECS volume fraction observed during wakefulness.

Norepinephrine and noradrenergic signaling

NE regulates the activity of neural circuits, coordinates state changes and adaptive responses to stimuli, wakefulness, vigilance, arousal, and has a role in mood and transient stress (Ruhé et al., 2007; Eduardo E. Benarroch, 2009; O'Donnell et al., 2012). Neurons in the locus coeruleus (LC) produce NE and send projections throughout the cortex. NE is released from varicosities along efferent projections, diffusing through the tissue to reach multiple targets (Bekar et al., 2012; O'Donnell et al., 2012; Schwarz and Luo, 2015). NE binds to a variety of adrenergic receptors (ARs) expressed throughout the brain, with expression varying both by brain region and by cell type (Joseph and Miller, 1988; Lerea and McCarthy, 1989; Hertz et al., 2010). Behavioral state affects the levels of tonic and phasic LC firing, resulting in different receptors being recruited since AR affinity for NE varies (Berridge and Waterhouse, 2003; Eduardo E. Benarroch, 2009; O'Donnell et al., 2012). NE signaling coordinates a whole organism to respond effectively to stimuli while in a particular state.

NE-binding ARs are GPCRs that involve several types of intracellular signaling pathways. α_1-ARs are G_q GPCRs that trigger intracellular Ca^{2+} release from internal stores (Jason J. Radley et al., 2008; O'Donnell et al., 2012; Nuriya et al., 2018). α_1-ARs are associated with enhancing neurotransmission and plasticity and have the highest NE binding affinity (Santana et al., 2013). α_2-ARs are $G_{i/o}$ GPCRs that reduce PKA activity and cAMP levels. α_2-ARs are associated with inhibitory effects, reducing NE release from LC projections and neuronal excitability (Scheinin et al., 1994; Tavares et al., 1996; Frances Davies et al., 2004; Hertz et al., 2010). Finally, $\beta_{1,2}$-ARs are G_s GPCRs that increase PKA activity and cAMP levels, and are usually associated with enhancing neuronal excitability and plasticity in certain circuits (Maity et al., 2015). $\beta_{1,2}$-ARs have

the lowest NE binding affinity (PA Rosenberg et al., 1994; Ji et al., 2008; Hertz et al., 2010; Grzelka et al., 2017). While α_1 and α_2-ARs can normally be stimulated by tonic levels and some phasic NE release, $\beta_{1,2}$-ARs are active during phasic NE release and higher NE concentrations (Hertz et al., 2010; O'Donnell et al., 2012).

NE is vital for the proper functioning of the nervous system, and aberrant NE signaling is associated with psychiatric disorders, neurodegenerative disorders and can impair learning and memory (Breier, 1990; Eduardo E. Benarroch, 2009; Moret and Briley, 2011; Gao et al., 2016). In both Alzheimer's and Parkinson's disease, loss of noradrenergic cells in the locus coeruleus, through an accumulation of tau or synuclein respectively, result in lower NE levels (Berridge and Waterhouse, 2003; Kalinin et al., 2007; Chalermpalanupap et al., 2018). It is thought NE hypofunction contributes to impaired cognition, memory and emotion processing (Ruhé et al., 2007; Moret and Briley, 2011; Durán et al., 2023). Depression has also been associated with impaired NE signaling. Ablating the locus coeruleus in rodent models results in depressive-like behavior, and NE levels are greatly reduced in some human patients with major depression (Ruhé et al., 2007; Moret and Briley, 2011; Chandley et al., 2013; Szot et al., 2016). One of the most effective antidepressants, serotonin norepinephrine reuptake inhibitors (SNRI), partly relies on increasing NE tone in the brain (Inazu et al., 2003; Kitayama et al., 2008; Moret and Briley, 2011). In the case of schizophrenia, NE hyperactivation may contribute to the positive symptoms suffered. In schizophrenic patients, NE levels are often elevated, and patients express more noradrenergic markers (Gottesman and Shields, 1967; Breier, 1990; Nagamine, 2020). Beyond that, medications meant to reduce NE activity help alleviate positive symptoms while noradrenergic agonists worsen those symptoms (Nagamine, 2020).

Norepinephrine signaling in astrocytes

For a long time, studies in NE signaling focused on neurons to understand how NE modulates circuit activity and behavior. However, astrocytes express multiple NE receptor subtypes on their fine processes, some of which are positioned near NE projections and a majority of which associate with synapses (Aoki et al., 1987; Salm and McCarthy, 1989; Duffy and Macvicar, 1995; Bekar et al., 2008; Hertz et al., 2010). Beyond just NE, astrocytes play an active role in mediating the effects of longer range diffusing, volume transmitted molecules, including monoamines (Hirase et al., 2014). Today, it's even proposed that astrocyte associations with neurons and responsiveness to monoamines make them the perfect effectors for monoaminergic activity, and to tune circuit activity (Paukert et al., 2014; Ma et al., 2016; Bazargani and Attwell, 2017). NE signaling has the potential to elicit astrocyte release of gliotransmitters such as D-serine, ATP and adenosine, which can drive excitability or inhibit activity (Gordon et al., 2005; Pankratov and Lalo, 2015; Ma et al., 2016). Ion homeostasis and $[K^+]_e$ can be altered by monoamines like NE, changing astrocyte K^+ clearance through affecting K^+ channels, Na^+K^+-ATPase and gap junction function (Song et al., 2015; Wotton et al., 2020). Modulating K^+ clearance aids in removing elevated $[K^+]_e$ that coincides with NE signaling and a state of wakefulness. This can have a broad effect on the excitability or inhibition of a circuit, and recovery from stimulation.

α_1 adrenergic receptors and astrocyte Ca^{2+} signaling

NE has been canonically linked to astrocyte Ca^{2+} signaling via α_1-AR activity (Salm and McCarthy, 1990; Duffy and Macvicar, 1995; Kirischuk et al., 1996; Bekar et

al., 2008; Paukert et al., 2014; Pankratov and Lalo, 2015). Astrocytes are electrically passive and do not conduct currents like neurons (Henneberger and Rusakov, 2012). Instead, the primary means of studying astrocyte physiology and activity is by observing Ca^{2+} events (Aguado et al., 2002; Hirase et al., 2004; Bernardinelli et al., 2011; Di Castro et al., 2011; Bindocci et al., 2017). NE and α_1-AR agonists stimulate the G_q GPCR signaling pathway, activating PLC to increase production of IP_3, which binds to endoplasmic reticulum IP_3R_2 (specific to astrocyte IP_3 receptor subtype) and triggers the release of stored Ca^{2+} (Bekar et al., 2008; Hertz et al., 2010; Srinivasan et al., 2015; Wahis and Holt, 2021). The number of Ca^{2+} events, along with duration and intensity, across an astrocyte's processes play a critical role in many astrocyte functions (Woo et al., 2012; Khakh and McCarthy, 2015; Bazargani and Attwell, 2016; Ye et al., 2017). Studies eliminating G_q GPCR signaling with IP_3R_2 knock out animals and removing Ca^{2+} signaling show the importance G_q GPCR Ca^{2+} signaling plays in gliotransmission, and astrocyte responses to local neuronal activity and volume transmitted monoamines (Takata et al., 2011; Srinivasan et al., 2015; Biesecker et al., 2016; Sherwood et al., 2017; Yu et al., 2018).

NE signaling tunes astrocytes to be more responsive to local glutamate activity in the somatosensory cortex, visual cortex and cerebellum (Paukert et al., 2014; Del Franco et al., 2022). For example, in awake behaving mice, local neuronal activity from visual stimulus does very little to elicit astrocyte Ca^{2+} signaling. However, when mice are aroused and running, increasing NE signaling, astrocyte Ca^{2+} events now reliably occur in response to a visual stimulus (Paukert et al., 2014; Gray et al., 2021). NE-increased astrocyte Ca^{2+} signaling is also associated with gliotransmission modulating neuronal activity (Gordon et al., 2005; Pankratov and Lalo, 2015; Ma et al., 2016). In zebrafish,

the sensation of moving but not going anywhere creates futility, causing a fish to eventually give up and stop swimming. The cognitive dissonance of swimming but not moving causes NE release to increase. Motor activity and swimming continues until high enough NE levels trigger astrocyte Ca^{2+} increases, resulting in ATP release (Mu et al., 2019). Astrocyte ATP then activates inhibitory neurons that then turn off motor circuits, and the fish stops swimming (Mu et al., 2019). As previously mentioned, astrocyte α_1-AR activity in the rodent hippocampus is associated with D-serine release, modulating the NMDAR activity during learning tasks and electric stimulation (Pankratov and Lalo, 2015).

β adrenergic receptors and astrocyte cAMP signaling

β-ARs are highly expressed by astrocytes as well (Salm and McCarthy, 1989; Hertz et al., 2010). The role of β-AR activity and increasing cAMP levels in astrocytes remains less understood compared to its α_1-AR counterpart. β-AR activity coincides with high NE levels from phasic LC firing, which happens in response to higher arousal and salient stimuli (O'Donnell et al., 2012). cAMP signaling through β-AR activity has been found to affect multiple astrocyte functions and neuronal signaling (PA Rosenberg et al., 1994; Laureys et al., 2010; Grzelka et al., 2017; Zhou et al., 2019).

While other ARs influence metabolism by stimulating glycogenesis to build energy stores, β-AR activity results in glycogenolysis and production of glucose (Subbarao and Hertz, 1990; Hertz et al., 2010; Zhou et al., 2019). This release of energy stores aptly occurs in response to the energy demands necessary for sustaining heightened states of activity and arousal. β-AR stimulation of astrocyte metabolic

processes and providing energy metabolites to neurons is critical for learning and memory in the hippocampus (Song et al., 2015; Gao et al., 2016).

ARs also modulate glutamate uptake. While NE enhances glutamate uptake through α_1-AR activity, activation of astrocyte β-ARs results in slightly reduced uptake (Hansson and Rönnbäck, 1991, 1992). Opposing effects from AR activity are also found with gap junction permeability. While α_1 and α_2-AR signaling reduces gap junction permeability, β-AR activity increases gap junction permeability (Giaume et al., 1991; Nuriya et al., 2018). Furthermore, K^+ clearance is enhanced through astrocyte β-ARs increasing Na^+K^+-ATPase activity, aiding in ion homeostasis and K^+ regulation (Song et al., 2015; Wotton et al., 2020).

β-AR activity mediates changes to astrocyte morphology, increasing process stellation in culture and process expansion in tissue. As previously mentioned, researchers observed β-AR agonist isoproterenol (ISO) increases astrocyte volume in rat visual cortex and proposed that these changes likely explain the ISO-mediated reduction of ECS volume fraction (Sherpa et al., 2016). Given that β-AR activity increases astrocyte process volume, glutamate spillover should be reduced alongside recruitment of extrasynaptic glutamate NMDAR activity.

Medial prefrontal cortex

Besides sensory cortical areas, the effect of β-AR activity on astrocyte process volume in other brain regions has gone unexplored. Astrocytes populations can be heterogenous in expression and function between different brain regions (Cavalcante et al., 1996; Poopalasundaram et al., 2000; Boulay et al., 2017; Lydie Morel et al., 2017; Minge et al., 2021). Some subtypes even appear within the same region. A region where

glutamate spillover and astrocyte β-AR activity could be particularly relevant to certain brain disorders is the mPFC. To illustrate how astrocyte function can vary between regions, glutamate transport differs between the somatosensory cortex and the anterior cingulate cortex (ACC), an area of emotion processing like the mPFC (Romanos et al., 2019). Extracellular glutamate is cleared at a much faster rate in the ACC compared to the somatosensory cortex, especially with increasing amounts of glutamate present from high-frequency stimulation. Limiting glutamate spillover is a critical function of astrocytes, especially in the frontal cortices (Romanos et al., 2019). Exploring the role of β-AR activity on astrocyte process volume and its ability to influence glutamate spillover in the mPFC could further our understanding of astrocyte contributions to neuronal activity.

The rodent mPFC is with associated executive function, playing a role in processing emotion, response to appetitive and aversive stimuli, learning and memory, social experience and behavior, by integrating cortical and subcortical inputs (Hoover and Vertes, 2007; Jason J. Radley et al., 2008; van Aerde and Feldmeyer, 2015). The mPFC can be separated into the prelimbic and infralimbic prefrontal cortex (Heidbreder and Groenewegen, 2003; Van De Werd et al., 2010). Both areas of the mPFC differentially affect elements of emotion processing. For example, while prelimbic activity promotes responsiveness to fear, infralimbic activity facilitates fear extinction (Heidbreder and Groenewegen, 2003; Jason J. Radley et al., 2008). The mPFC is densely innervated by monoaminergic projections, including dopamine (DA), serotonin (5-HT) and NE, all of which are crucial for mPFC function (Hoover and Vertes, 2007; Santana and Artigas, 2017).

Unlike somatosensory regions, the mPFC does not have a defined Layer 4 for receiving afferent information (van Aerde and Feldmeyer, 2015; Santana and Artigas,

2017). Instead, the mPFC has an expanded Layer 5 consisting of two major pyramidal neuron subtypes, depending on their efferent projections (Dembrow and Johnston, 2014; Moberg and Takahashi, 2022). There are intratelencephalic (IT) neurons that project to cortical and striatal targets, and extratelencephalic (ET) neurons that project to subcortical regions like monoaminergic nuclei, in addition to cortical targets (Dembrow and Johnston, 2014; van Aerde and Feldmeyer, 2015). Thalamic and long-range feedback connections are extensively made to L1 dendrites, while cortical, thalamic and subcortical regions project throughout L1 – L5 (Kuroda et al., 1998; Hoover and Vertes, 2007). Similarly, monoaminergic projections and receptors are found in all the layers of the mPFC (Santana and Artigas, 2017). This includes NE, where most studies have focused on neuronal activity. NE has been shown to influence neuronal excitability through binding to pre- and postsynaptic receptors (Jason J. Radley et al., 2008; Ji et al., 2008; Grzelka et al., 2017). While astrocytes have been shown to express β-ARs in other emotion processing regions of the brain like the ACC, expression in the mPFC has not been explored (Gao et al., 2016).

mPFC dysfunction is found in several psychiatric disorders. More specifically, some behavioral deficits have been linked to aberrant NE activity and excessive extrasynaptic NMDAR activity in the mPFC. NE dysfunction and disturbed signaling in the mPFC affects multiple psychiatric disorders, ranging from neurodegenerative diseases to major depression and schizophrenia (Breier, 1990; Kitayama et al., 2008; Eduardo E. Benarroch, 2009; Szot et al., 2016; Nagamine, 2020). In most cases, disruption occurs from reduced NE levels (Moret and Briley, 2011; Chandley et al., 2013; Szot et al., 2016; Chalermpalanupap et al., 2018; Durán et al., 2023). Meanwhile, glutamate spillover in the mPFC has also been associated with a range of similar

disorders (Zhao et al., 2016; Li et al., 2018). In rodents exposed to chronic unpredictable stress that developed depressive-like behavior, higher levels of extracellular glutamate were detected in the mPFC, along with enhanced extrasynaptic GluN2B NMDAR activity (Li et al., 2018). Another study that blocked glutamate transport in the awake rat prefrontal cortex, probably inducing glutamate spillover in the process, resulted in the development of anhedonia towards sucrose water (John et al., 2012). Anhedonia is a state of disinterest towards things that used to bring pleasure and is commonly found in major depression and other disorders affecting mPFC activity. GluN2B NMDAR activity has been linked to depressive-like behavior and that blocking these extrasynaptic enriched receptors results in anti-depressant effects (Miller et al., 2014, 2017; Tang et al., 2020; Shi et al., 2021). Reduced glutamate transporter expression and astrocyte volume in individuals with major depression and rodent models of depression coincide with the detrimental effects of glutamate spillover and extrasynaptic NMDAR activity in the mPFC (John et al., 2012; Kiss et al., 2012; Rajkowska and Stockmeier, 2013; Zhao et al., 2016; Li et al., 2018; Codeluppi et al., 2021).

Summary

Astrocytes play a vital role at the synapse, regulating glutamate activity and limiting spillover (Rusakov, 2001; Huang and Bordey, 2004; Hires et al., 2008). Through the dynamic morphology of their fine processes, astrocyte volume can change under several conditions, many of which have been shown to influence glutamate spillover (Piet et al., 2004; Henneberger et al., 2020; Popov et al., 2020). Glutamate can reach extrasynaptic NMDARs, whose excessive activation elicits negative consequences (Hardingham et al., 2002; McCullumsmith and Sanacora, 2015). NE may be able to

impact glutamate spillover through its ability to remodel astrocyte processes and reduce ECS volume fraction (Xie et al., 2013; Sherpa et al., 2016), which have been shown to affect glutamate spillover in other systems (Piet et al., 2004; Sykova, 2004; Kinney et al., 2013). NE acts on several receptors, affecting astrocyte and neuronal physiology, and whose disruption can lead to several disorders (Eduardo E. Benarroch, 2009; Hertz et al., 2010; O'Donnell et al., 2012; Wahis and Holt, 2021). NE-mediated β-AR activity impacts astrocyte morphology, increasing process volume in sensory cortical areas (Sherpa et al., 2016).

However, β-AR activity changing astrocyte volume in the mPFC has not been investigated. The mPFC is a region of the brain densely innervated by NE inputs and is responsible for emotion processing and execution function (Jason J. Radley et al., 2008; Santana and Artigas, 2017). Dysregulation of NE signaling and extrasynaptic NMDAR activity in the mPFC have been associated with mood and psychiatric disorders (Breier, 1990; Ruhé et al., 2007; Szot et al., 2016; Li et al., 2018; Tang et al., 2020). The impact β-AR-mediated changes to astrocyte volume can have on glutamate spillover and NMDAR activity are also unexplored. Both questions are extremely relevant to the mPFC and may provide insight into other mechanisms at play in certain brain disorders.

Therefore, we investigated the role astrocyte β-AR activity played in the mPFC, looking at its effects on astrocyte volume and on pyramidal neuron NMDAR signaling. To expand our knowledge of noradrenergic effects on astrocyte volume, we tested the hypothesis that NE and β-AR signaling increase astrocyte process volume in the previously unexplored mPFC. Prior studies found that changes to astrocyte volume affect glutamate spillover, where increasing astrocyte volume reduces glutamate spillover and extrasynaptic NMDAR recruitment. Therefore, we tested the hypothesis

that β-AR signaling reduces pyramidal neuron NMDAR activity, including extrasynaptic NMDARs, in an astrocyte-dependent manner. By testing how NE activity influences extrasynaptic NMDAR signaling in the mPFC, these hypotheses aim to further our understanding of potential mechanisms involved in a multitude of psychiatric disorders.

Chapter 2: Astrocyte β-adrenergic receptor activity regulates NMDA receptor signaling of medial prefrontal cortex pyramidal neurons

Introduction

Proper functioning of the nervous system relies on tight regulation of glutamate neurotransmission. Astrocytes serve a critical role in this process and carry out various functions vital to synaptic physiology through their complex interactions with glutamatergic synapses (Araque et al., 1999b; Oliet et al., 2001; Rusakov, 2001; Halassa et al., 2007b; Theodosis et al., 2008). Peripheral astrocyte processes (PAPs) closely associate with synapses, acting as the primary means of glutamate uptake and as barriers to diffusion from the synaptic cleft (Rusakov, 2001; Huang and Bordey, 2004; Takayasu et al., 2006; Nie and Weng, 2009). As such, astrocytes play a critical role in regulating the extent to which non-synaptic receptors are activated following glutamate release. In addition to being expressed in the postsynaptic density, NMDA receptors (NMDARs) are often found in extrasynaptic sites (Harris and Pettit, 2008; Papouin et al., 2012). Glutamate spillover and recruitment of these extrasynaptically located NMDARs is important under various physiological and pathological conditions (Hardingham et al., 2002; Zhang and Sulzer, 2003; Oliet et al., 2004; Delgado et al., 2018).

Astrocyte morphology is dynamic and can drive changes in the extracellular space (ECS), affecting neurotransmitter diffusion from the synapse. PAP morphology is modulated by norepinephrine (NE) (Xie et al., 2013; Sherpa et al., 2016), serotonin (Müller et al., 2021), oxytocin (Theodosis and Poulain, 2001), long term plasticity (LTP) induction (Perez-Alvarez et al., 2014; Henneberger et al., 2020), fear memory induction (Badia-Soteras et al., 2022), caloric restriction (Popov et al., 2020), and sleep-wake cycles (Xie et al., 2013). Studies that observed PAP retraction and reduced astrocyte

process volume noted enhanced glutamate spillover and NMDAR activation. Conversely, astrocyte process volume increases led to decreased extrasynaptic NMDAR recruitment (Popov et al., 2020). NE was found to expand PAPs and increase process volume (Vardjan et al., 2014; Sherpa et al., 2016), though its effects on glutamate spillover remain unexplored.

NE modulates the activity of neural circuits, coordinating state changes and adaptive responses to stimuli, wakefulness, arousal, mood, and stress (Eduardo E. Benarroch, 2009; Schwarz and Luo, 2015). Various adrenergic receptor (AR) subtypes are expressed on astrocytes, though most prior work has focused on Ca^{2+} signaling elicited by G_q G-protein coupled receptor (GPCR) α_1-AR activity (Bekar et al., 2008; Paukert et al., 2014; Tran et al., 2018). Astrocytes also express G_s-GPCR β-ARs (Hertz et al., 2010). β-AR activity enhances metabolic support, K^+ uptake, gap junction connectivity, as well as changes in morphology (Giaume et al., 1991; PA Rosenberg et al., 1994; Laureys et al., 2010; Sherpa et al., 2016; Wotton et al., 2020). Despite evidence that NE and β-AR activity affect astrocyte volume in sensory cortices, the effect of NE has not been tested in emotion processing brain regions where noradrenergic and NMDAR signaling dysfunction result in multiple psychiatric disorders (Breier, 1990; Ruhé et al., 2007; Li et al., 2018; Uno and Coyle, 2019; Tang et al., 2020). Nor has the link between noradrenergic signaling and glutamate spillover been explored.

We have now investigated the role of β-AR activity on astrocyte volume in an emotion processing region of the brain with a high degree of noradrenergic innervation, the medial prefrontal cortex (mPFC) (Santana and Artigas, 2017), characterizing its effects on pyramidal neuron NMDAR signaling. We show that NE and the β-AR agonist isoproterenol (ISO) increase astrocyte volume in the mPFC and demonstrate that these

changes can be blocked by eliminating astrocyte GPCR signaling. We also find that ISO reduces NMDAR post-synaptic currents (EPSCs) associated with glutamate spillover. Blocking astrocyte responsiveness to ISO reversed this reduction of NMDAR EPSCs. Finally, by pharmacologically blocking synaptic NMDARs, we confirmed that ISO reduced extrasynaptic NMDAR EPSCs.

Methods

Ethics Statement

All experimental procedures were approved by and adhered to the guidelines of the Institutional Animal Care and Use Committee of the University of Minnesota.

Brain Slice Preparation

All experiments used tissue harvested from 5 to 12 weeks old male and female C57BL/6 mice. Mice were anaesthetized with isoflurane and decapitated for rapid removal of the brain. 350 μm coronal brain slices of the mPFC were taken in oxygenated (95% O_2, 5% CO_2) and chilled sucrose artificial CSF (aCSF). Brain slices were initially incubated in 32°C aCSF with 0.5 μM sulforhodamine 101 (SR 101; S7635, Sigma-Aldrich) for 10 min to label astrocytes. Slices then recovered in 32°C aCSF for another 20 min and another 30 min in room temperature aCSF until experiments were conducted. During experiments, a single brain slice was transferred to an immersion recording chamber and held stationary by a harp. Slices were perfused with oxygenated, room temperature aCSF solutions at 2.5 ml/min.

Measurement of changes in astrocyte volume

Astrocytes were whole-cell patch-clamped and filled with a fluorescent dye to measure changes in process volume. Layer 2/3 astrocytes were identified based on their labeling by SR 101, small soma size (5 – 10 μm), hyperpolarized V_{rest} (-80 mV), and distinct morphology (Bushong et al., 2002; Henneberger and Rusakov, 2012; Minge et al., 2021). Astrocytes were filled for 25 min with the gap junction-impermeant dye Alexa Fluor 488 (3,000 MW) dextran (40 μM; D34682, Invitrogen) prior to the start of recordings. The dye equilibrated through the finer astrocyte processes during this time (Fig. 1A, B). Using a gap junction-impermeant dye eliminated the possibility that observed fluorescent intensity changes were due to diffusion of dye into other astrocytes through gap junctions (Giaume et al., 1991). The fine processes of astrocytes fall below the imaging resolution of confocal microscopy and dye-filling provides a method of measuring process volume, where fluorescence is proportional to the space occupied by the processes (Henneberger et al., 2020). By comparing the relative brightness of dye-filled processes to baseline fluorescence established prior to an experimental manipulation, observed changes in fluorescence will be proportional to changes to astrocyte process volume.

We captured single focal plane images of a dye-filled astrocyte at four-minute intervals. The z-axis was manually adjusted to adjust for drift over the recording period. Dye-filled astrocytes were imaged using confocal microscopy (Olympus, FV1000) through a 40x, 1.00 numerical aperture (NA) water objective to acquire, 512 x 512 pixel images (0.155 x 0.155 μm pixels). Three images were acquired and averaged together every four minutes for 20 min in control aCSF to establish a baseline and then for an additional 40 min with either NE (20 μM; A0937, Sigma-Aldrich), ISO (5 μM; I5627, Sigma-Aldrich), or control aCSF. In some experiments, astrocytes were patched with an

internal solution containing GDPβS (100 μM; ALX-480-056, Enzo Life Sciences) to block noradrenergic receptor G-protein activity (Navarrete et al., 2012; Anna Cavaccini et al., 2020).

Sequences of images were registered using a custom MATLAB (2016b) program, then analyzed with Fiji ImageJ. A manual ROI was drawn to encompass filled astrocyte processes (Fig. 1C – F) and the averaged ROI fluorescence was calculated for each time point (Fig 1G, H). Fluorescence values are reported relative to the baseline fluorescence,

$$\text{Change in Fluorescence from Baseline (\%)} = 100 * (F_t - F_{Baseline}) / F_{Baseline}$$

Measurement of neuronal NMDA and AMPA receptor currents

Layer 5 mPFC pyramidal neurons were patched to record evoked EPSCs. Large-soma cells, 300 – 500 μm from the midline, were whole-cell patch-clamped and filled with Alexa Fluor 594 Hydrazide dye (40 μM; A10438, Invitrogen). Neurons were imaged with confocal microscopy to confirm the identity of the patched cell, based on a prominent apical dendrite (Fig. 2A). Cells with series resistance (R_s) > 20 MΩ were excluded from analysis. To evoke EPSCs, a theta-glass pipette (BT-150-10, Sutter Instrument) delivered electric stimuli to Layer 2/3, ~150 μm from the patched neuron's apical dendrite (Fig. 2A). Single 100 μs current pulses were delivered through a stimulator (A-M Systems Isolated Pulse Stimulator 2100) and the current amplitude adjusted to elicit 40 – 260 pA EPSCs. Ten stimuli bursts were delivered at 50 Hz to elicit glutamate spillover and recruit extrasynaptic NMDARs (Harris and Pettit, 2008). EPSC traces were zeroed to baseline current and for illustration were smoothed by a 3 ms moving average filter using MATLAB. Patch clamp experiments and stimuli were

recorded and controlled using a MultiClamp 700b amplifier (Molecular Devices) and LabChart (ADInstruments). Currents were sampled at 10 kHz and filtered at 3 kHz and R_s compensated to ~70%. EPSCs were analyzed using custom MATLAB programs.

Measurement of NMDAR EPSCs. NMDAR currents were isolated by blocking AMPARs and $GABA_A$Rs with CNQX (10 μM; Cat. No. 1045, Tocris) and gabazine (5 μM; 5059860001, Sigma-Aldrich), respectively. Patched neurons were voltage-clamped and held at +40 mV to free NMDAR Mg^{2+} block. Five – 10 single EPSCs were averaged together and 2 – 4 trials of 10 stimuli EPSCs were averaged together. EPSC peak amplitude from 10 stimuli bursts was measured after the 10^{th} stimulus. EPSC charge transfer was calculated as the area under the trace beginning from the current peak to the end of single EPSC recordings, and for 1.6 s after the evoked current peak of the 10^{th} stimulus for 10 stimuli EPSCs. At the end of an experiment, currents were blocked with D-AP5 (50 μM; Cat. No. 0106, Tocris) to verify that they were NMDAR EPSCs.

Measurement of 10 stimuli NMDAR EPSC decay constant. The decay constant of NMDAR EPSCs evoked by 10 stimuli bursts were calculated by fitting the EPSC decay after the 10^{th} evoked EPSC with a double exponential using the MATLAB curve fitting tool. The fast decay constant component (τ_f) was compared between control aCSF and ISO recordings.

Measurement of AMPAR EPSCs. We assessed whether ISO affected glutamate release and synaptic activity by measuring AMPAR EPSCs (Ji et al., 2008; Grzelka et al., 2017). AMPAR currents were isolated by blocking NMDARs with D-AP5 (50 μM). Neurons were voltage-clamped and held at the Cl^- reversal potential, ~-52 mV (after correcting for the liquid junction potential), to eliminate the $GABA_A$R contribution to the evoked currents. AMPAR current isolation was confirmed by using CNQX (10 μM) to

eliminate AMPAR EPSCs. For AMPAR EPSCs evoked by 10 stimuli, the peak EPSCs evoked by each stimulus were summed together to reflect the overall synaptic glutamatergic activity, Σ AMPAR EPSCs.

Evaluation of the role of astrocyte β*-adrenergic receptor activity on EPSCs.* We eliminated astrocyte β-AR-mediated changes to EPSCs by loading the astrocyte network near the recorded neuron with the gap junction-permeable, G-protein blocker GDPβS (Navarrete et al., 2012; Anna Cavaccini et al., 2020). An astrocyte in Layer 2/3, ~50 µm from the stimulus electrode was patched and loaded with an internal solution containing 100 µM GDPβS and the gap junction-permeable dye Alexa Fluor 488 Hydrazide (40 µM; A10436, Invitrogen) to verify spread of GDPβS. Astrocytes were filled for 30 minutes before removing the patch pipette. Immediately afterwards, a Layer 5 pyramidal neuron was patched and imaged to confirm that its dendrites fell within the region of the GDPβS-filled astrocytes (Fig. 2A).

Measurement of *extrasynaptic NMDA receptor currents*

We investigated the extent to which ISO reduces extrasynaptic NMDAR currents. Single and 10 stimuli NMDAR EPSCs were initially recorded in aCSF at +40 mV. The preparation was then perfused with the activity-dependent NMDAR blocker MK-801 (25 µM; M107, Sigma-Aldrich) (Huettner and Bean, 1988; Harris and Pettit, 2008; Papouin et al., 2012; Yang et al., 2017). Single stimuli were delivered at 1 Hz for 10 min, resulting in the block of synaptic NMDARs (Harris and Pettit, 2008; Papouin et al., 2012). MK-801 was then washed out for 15 min while the neuron was held at -60 mV to prevent further NMDAR activation. Recordings were not included if the post MK-801 single stimulus

EPSCs were greater than 15% of the pre MK-801 EPSCs or if the post MK-801 EPSCs in ISO increased by more than 50% after switching from the post MK-801 aCSF.

Solutions and drugs

Brains were sliced in a sucrose solution that contained (in mM): 228 Sucrose, 1 NaH_2PO_4, 2.5 KCl, 7 $MgCl_2$, 11 glucose, 0.5 $CaCl_2$, 0.4 sodium ascorbate, 26 $NaHCO_3$, bubbled with 95% O_2/5% CO_2, (pH 7.35; 300–310 mOsm). aCSF used for recovery and recordings contained (in mM): 125 NaCl, 1.25 NaH_2PO_4, 2.5 KCl, 1.5 $MgCl_2$, 20 glucose, 1.2 $CaCl_2$, 0.5 $_L$-glutamine, 0.4 sodium ascorbate, 26 $NaHCO_3$, bubbled with 95% O_2/5% CO_2, (pH 7.35; 300–310 mOsm). The patch pipette solution for patching astrocytes contained (in mM): 120 K-gluconate, 4.5 $MgCl_2$, 9 HEPES, 0.1 EGTA, 14 tris$_2$-phosphocreatine, 4 Na_2-ATP, 0.3 tris-GTP, sucrose to bring the solution to 280 – 290 mOsm, pH 7.25. Astrocyte internal included either 40 μM Alexa Fluor 488 Dextran (3,000 MW) for astrocyte volume recordings or 40 μM Alexa Fluor 488 Hydrazide to track GDPβS diffusion for neuronal recordings. For experiments blocking astrocyte GPCR activity, tris-GTP was replaced with 100 μM GDPβS. The patch pipette solution for patching pyramidal neurons contained (in mM): 105 Cs-methanesulfonate, 10 TEA-Cl, 20 HEPES, 10 EGTA, 2 QX-314 Cl^-, 5 Mg-ATP, 0.5 tris-GTP, sucrose to bring the solution to 280 – 290 mOsm, pH 7.25. Neuronal internal solution included 40 μM Alexa Fluor 594 Hydrazide.

Statistics and Analysis

Two sample t-tests, paired and unpaired, and two-way ANOVAs were used, as appropriate. Data are expressed as mean ± SEM in the text and figures. The sample

size (n) of cells and animals for each group are reported throughout the text. The sample size for each group was sufficiently powered (0.8) when estimating a moderate effect size of 0.15 and the null-hypothesis rejection was $\alpha = 0.05$. Effect size was based on estimates from comparable studies investigating astrocyte volume, changes to glutamate spillover, and extrasynaptic NMDAR activity (Henneberger et al., 2020; Popov et al., 2020). A two-way ANOVA with Tukey-Kramer multiple comparisons post hoc test was conducted on astrocyte volume changes measured after 40 min perfusion with experimental or control solutions, and intracellular GDPβS. Student's Paired t-tests were run between normalized control and ISO EPSC recordings. Unpaired t-tests were used to compare the effects of normalized ISO responses between neuron EPSCs with or without GDPβS-loaded astrocytes. Two-way ANOVA with Tukey-Kramer post hoc was used to compare fast decay time constants between NMDAR currents in control and ISO, and the presence of GDPβS-loaded astrocytes. Data analysis and statistics were carried out using custom MATLAB scripts. The data, images and MATLAB scripts for analysis and statistics will be made available upon request.

Results

Norepinephrine and β-adrenergic agonists increase astrocyte volume in the medial prefrontal cortex

Noradrenergic activity alters astrocyte morphology and process volume in certain brain regions (Xie et al., 2013; Vardjan et al., 2014; Sherpa et al., 2016). We wanted to determine whether similar morphological changes occur in the mPFC, which receives a large amount of noradrenergic input. We used a previously-established technique to measure process volume, filling astrocytes with a gap junction-impermeant fluorescent dye and imaging dye-filled cells using confocal microscopy (Henneberger et al., 2020;

Minge et al., 2021). Fine astrocyte processes can be loaded with dye (Fig. 1A) while being restricted to the patched astrocyte (Fig. 1B). Compared to a stable baseline fluorescence, any change in process fluorescence represents a change in volume. Single images of process fluorescence prior to β-AR agonist ISO exposure (Fig. 1C) and after 40 min in ISO (Fig. 1D) highlight how astrocyte process fluorescence increases following ISO incubation (Fig. 1C – D, G). ISO increased process fluorescence by ~18% after 40 min exposure (18.41 ± 3.60% increase; n = 7 cells from 5 mice) (Fig. 1J). Incubating brain slices with NE for 40 min also increased the fluorescence in processes by ~18% (17.7 ± 2.4% increase; n = 7 cells from 7 mice) (Fig. 1J). Process volume increased significantly with both NE and ISO compared to control recordings measured after 40 min in aCSF (2.21 ± 1.86% increase; n = 8 cells from 8 mice) (ISO vs aCSF; ***$p = 2.43 \times 10^{-5}$; Tukey-Kramer post hoc, 2-way ANOVA) (NE vs aCSF; *** $p = 4.94 \times 10^{-5}$; Tukey-Kramer post hoc, 2-way ANOVA) (Fig. 1J).

We sought to determine whether the noradrenergic agonist effect on astrocyte process volume could be attributed to the agonists acting directly on astrocytes. To selectively eliminate noradrenergic signaling in astrocytes, we blocked GPCR signaling by loading dye-filled astrocytes with GDPβS, a G-protein inhibitor (Navarrete et al., 2012; Anna Cavaccini et al., 2020). Single images of process fluorescence from an astrocyte loaded with GDPβS prior to ISO exposure (Fig. 1E) and after 40 min in ISO (Fig. 1F) demonstrate that ISO exposure does not increase process fluorescence of GDPβS-filled astrocytes (Fig. 1E – F, H). Instead, while process fluorescence increases with ISO over time, the fluorescence increase is severely blunted by GDPβS, becoming no different from astrocyte fluorescence changes recorded in aCSF (Fig. 1I).

Relative changes in astrocyte process fluorescence are summarized in Figure 1J. Process fluorescence changes were significantly smaller after 40 min in NE for GDPβS-loaded astrocytes (4.97 ± 0.99% increase, n = 7 cells from 6 mice) or 40 min in ISO (0.47 ± 1.49% increase, n = 7 cells from 6 mice) compared to astrocytes lacking GDPβS loading (NE vs NE GDPβS; **$p = 1.39 \times 10^{-3}$; Tukey-Kramer post hoc, 2-way ANOVA) (ISO vs ISO GDPβS; ***$p = 6.96 \times 10^{-6}$; Tukey-Kramer post hoc, 2-way ANOVA) (Fig. 1J). Indeed, GDPβS loaded astrocyte process fluorescence in either noradrenergic agonist was similar to the fluorescence changes recorded in control aCSF (aCSF vs NE GDPβS; n.s., p = 0.926; Tukey-Kramer post hoc, 2-way ANOVA) (aCSF vs ISO GDPβS; n.s., p = 0.990; Tukey-Kramer post hoc, 2-way ANOVA) (Fig. 1J). We also verified that GDPβS by itself does not alter astrocyte process volume (aCSF GDPβS, 3.84 ± 0.65% increase, n = 7 cells from 6 mice) (aCSF vs aCSF GDPβS; n.s., p = 0.992; Tukey-Kramer post hoc, 2-way ANOVA) (Fig 1J). These results indicate that activation of β-ARs expressed on mPFC astrocytes elicit increases in process volume.

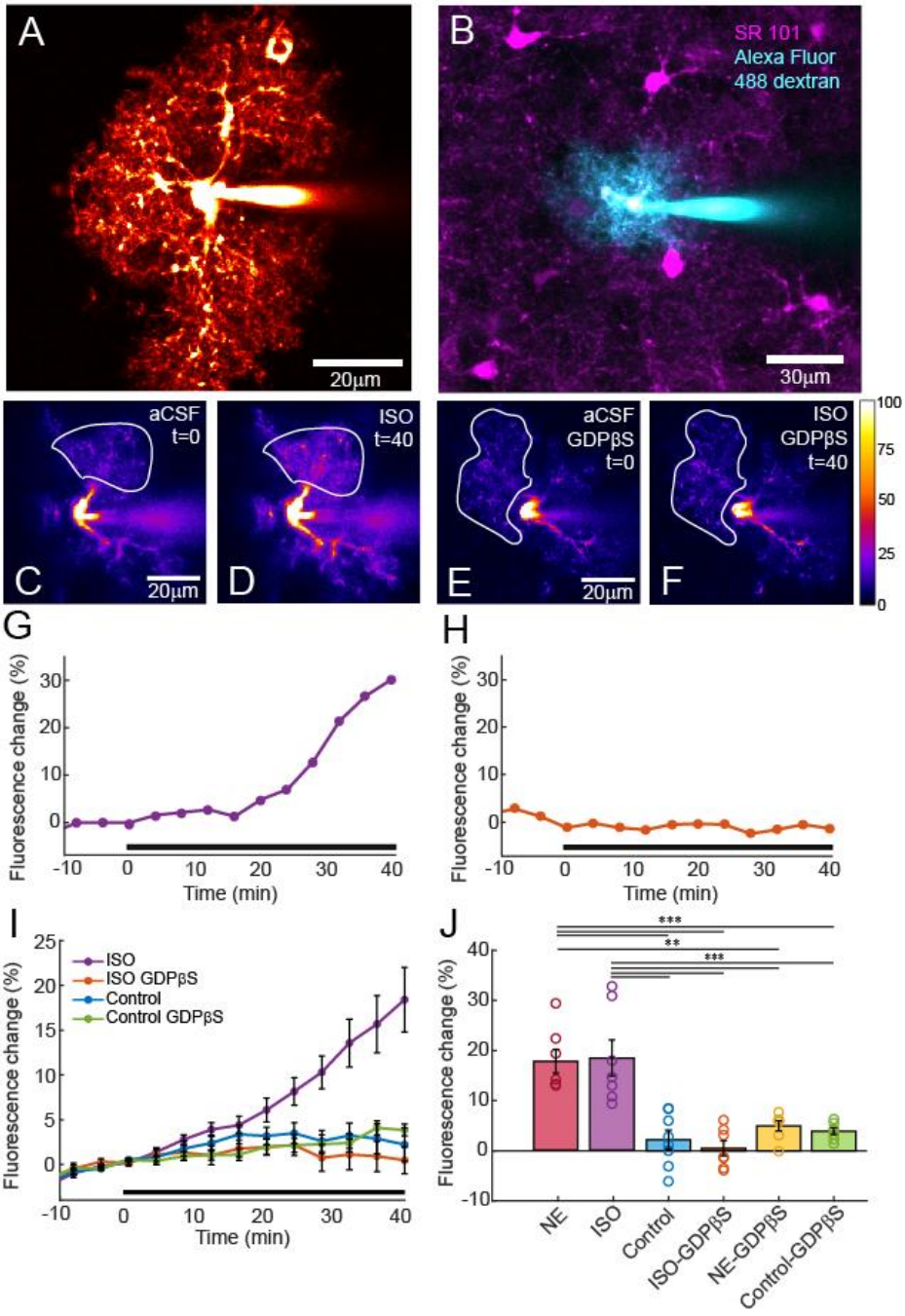

Figure 1. Noradrenergic agonists increase astrocyte process volume in the mPFC. **A,** Confocal image of an astrocyte filled with Alexa Fluor 488 dextran (3,000 MW). **B**, Confocal image of multiple astrocytes labeled with SR 101 (magenta) and a single astrocyte filled with Alexa Fluor 488 dextran (cyan). The Alexa Fluor dye does not spread

beyond the patched cell. **C – F,** Example fluorescence images of two dye-filled astrocytes. **C and D,** β-AR agonist ISO increases fluorescence intensity in the processes of an astrocyte. **C,** Last time point in aCSF. **D,** 40 min in ISO. **E and F,** Fluorescence intensity remains unchanged in an astrocyte loaded with GDPβS. **E,** Last time point in aCSF. **F,** 40 min in ISO. Pseudocolor scale indicates fluorescence intensity in arbitrary units. **G,** Astrocyte process brightness vs time from the experiment illustrated in C and D. **H,** Process brightness vs time for an astrocyte loaded with GDPβS, illustrated in E and F. In G and H, process brightness is measured in the ROIs indicated in C – F; the black bars indicate the time course of ISO incubation. **I,** Mean ± SEM astrocyte process fluorescence vs time for astrocytes initially in aCSF and exposed to experimental solutions for 40 min (black bar). Experimental solutions include ISO (purple), ISO with GDPβS-filled astrocyte (orange), aCSF control (blue), and aCSF control with GDPβS (green). **J,** Summary of astrocyte process fluorescence changes measured after 40 min incubation in noradrenergic agonists or control solution, with or without GDPβS loading of astrocytes. Mean ± SEM and data from individual cells are shown. NE (17.7 ± 2.4% increase; n = 7 cells from 7 mice), ISO (18.41 ± 3.60% increase; n = 7 cells from 5 mice), control aCSF (2.21 ± 1.86% increase; n = 8 cells from 8 mice), ISO-GDPβS (0.47 ± 1.49% increase, n = 7 cells from 6 mice), NE-GDPβS (4.97 ± 0.99% increase, n = 7 cells from 6 mice), aCSF-GDPβS (3.84 ± 0.65% increase, n = 7 cells from 6 mice). 2-way ANOVA with Tukey-Kramer post hoc multiple comparisons, *$p < 0.05$, **$p < 0.01$, ***$p < 0.001$. Exact p values contained within the text.

Astrocyte β-adrenergic receptor signaling reduces NMDA receptor activation

Since astrocyte volume changes influence glutamate signaling and NMDAR activity, we next sought to understand how β-AR signaling affected NMDAR activity (Oliet et al., 2004; Müller et al., 2021; Badia-Soteras et al., 2022). We used electrical stimulation of afferents in Layer 2/3 to evoke Layer 5 pyramidal neuron NMDAR currents (Fig. 2A). Single stimulus-evoked NMDAR EPSCs remain unchanged by ISO (Fig. 2B, F – G). Single stimulus-evoked NMDAR EPSC peak amplitude in ISO was unchanged in aCSF (0.88 ± 0.06; n = 7 cells from 6 mice, paired t-test, n.s., p = 0.10) as was NMDAR EPSC charge transfer in ISO (0.91 ± 0.12; n = 7 cells from 6 mice, paired t-test, n.s., p = 0.50) (Fig. 2F, G).

We then elicited NMDAR EPSCs using a 10 stimulus, 50 Hz burst, a stimulus paradigm associated with glutamate spillover and extrasynaptic receptor recruitment (Harris and Pettit, 2008) (Fig. 2C). Although there was no difference observed with single stimulus EPSCs in ISO, ISO significantly reduced high-frequency, repetitive stimulus-evoked NMDAR currents (Fig. 2C). ISO reduced the peak amplitude of these EPSCs by 18% (0.82 ± 0.03; n = 7 cells from 6 mice, paired t-test, ***p = 5.04 x 10^{-4}) and reduced the NMDAR EPSC tail charge transfer by 22% (0.78 ± 0.04; n = 7 cells from 6 mice, paired t-test, **p = 2.39 x 10^{-3}). For both single- and repetitive-stimuli, the NMDAR blocker D-AP5 reduced evoked currents by over 90% compared to control, confirming that we were measuring NMDAR currents in these recordings (Fig. 2B – C, F – G; 1 stimulus, 0.08 ± 0.01; n = 7 cells from 5 mice, paired t-test, ***p = 7.30 x 10^{-11}); (10 stimuli, 0.06 ± 0.01; paired t-test, ***p = 1.69 x 10^{-11}).

While ISO-induced astrocyte volume increases (Fig. 1J) may influence neuronal signaling, changes to neuronal NMDAR currents may also be due to direct action of ISO

on neurons, which also express β-ARs (Ji et al., 2008; Grzelka et al., 2017). We evaluated the role of astrocytes in the ISO effect on NMDAR EPSCs by blocking astrocytic β-AR signaling. Prior to recording neuronal NMDAR currents, we patched and loaded the astrocyte network with GDPβS (Fig. 2A) to selectively block astrocyte β-AR signaling and eliminate process volume increases (Fig. 1J). The spread of GDPβS from the patched astrocyte (Fig. 2A, asterisk) was tracked with a gap junction-permeable Alexa Fluor 488 to ensure astrocyte loading (Fig. 2A, arrowheads) near the recorded neuron.

The effect of ISO in reducing NMDAR currents was blocked when astrocytes were loaded with GDPβS, demonstrating that ISO modulation of NMDAR synaptic transmission is mediated, at least in part, by astrocytes. Consistent with the lack of effect of ISO on single-stimulus-evoked NMDAR currents, single stimulus-evoked NMDAR EPSCs were unchanged between control aCSF and ISO recordings with astrocyte GDPβS loading, both when measuring peak EPSC amplitude (1.07 ± 0.06; n = 7 cells from 7 mice, paired t-test, n.s., p = 0.265), and for charge transfer (1.17 ± 0.13; n = 7 cells from 7 mice, paired t-test, n.s., p = 0.255) (Fig. 2D, F – G). However, the impact of ISO on NMDAR EPSC peak amplitude varied when comparing the absence to the presence of GDPβS-loaded astrocytes in ISO; ISO elicited larger normalized peak amplitudes with GDPβS-loaded astrocytes (no GDPβS ISO vs GDPβS ISO; unpaired t-test, *p = 0.044) (Fig. 2E, F). GDPβS had no impact on the effect of ISO on NMDAR EPSC charge transfer (no GDPβS ISO vs GDPβS ISO; unpaired t-test, p = 0.18), however (Fig. 2G).

Loading astrocytes with GDPβS significantly enhanced repetitive stimulus-evoked NMDAR EPSCs when ISO was applied. When astrocytes were loaded with

GDPβS, ISO increased the peak NMDAR EPSC evoked by 10 stimuli by 30% compared to responses in control aCSF (1.30 ± 0.10; n = 7 cells from 7 mice, paired t-test, *p = 0.025) (Fig. 2F), though charge transfer remained unchanged (1.16 ± 0.10; n = 7 cells from 7 mice, paired t-test, n.s., p = 0.16) (Fig. 2G). Compared to ISO recordings done without GDPβS loading of astrocytes, where ISO reduced repetitive stimulus-evoked NMDAR EPSCs, when loaded with GDPβS ISO significantly enhanced repetitive stimulus-evoked NMDAR EPSC peak amplitude (no GDPβS ISO vs GDPβS ISO; unpaired t-test, ** $p = 2.64 \times 10^{-3}$) (Fig. 2F) and charge transfer (no GDPβS ISO vs GDPβS ISO; unpaired t-test, **$p = 8.34 \times 10^{-3}$) (Fig. 2G). Blocking astrocyte β-AR activity with GDPβS reversed the effect of ISO on repetitive stimulus-evoked NMDAR EPSCs. Results for all normalized NMDAR responses are summarized in Figures 2F and 2G. While ISO previously reduced 10 stimuli-evoked peak EPSC and charge transfer, the addition of GDPβS to astrocytes led to ISO greatly enhancing peak EPSC and charge transfer. Meanwhile, single stimulus EPSC measures remained largely unchanged.

As a control for loading of the astrocyte network, three of the seven cells from the no GDPβS recordings were conducted with astrocytes loaded with a standard astrocyte internal solution. There were no differences between ISO responses of single or 10 stimuli-evoked NMDAR EPSCs compared to control, whether astrocytes were patched with a control internal or not patched at all (unpaired t-test, n.s., $p > 0.38$ for all measures).

The decay time constant (τ) of repetitive stimulus-evoked NMDAR EPSCs has been shown to change with altered glutamate uptake and other properties affecting dwell time of glutamate near receptors (Diamond, 2005; Nie and Weng, 2009; Anderson et al., 2015). Since ARs can alter glutamate transport in astrocytes (Hansson and Rönnbäck,

1991, 1992), we compared ISO and control aCSF decay time constants for 10 stimulus-evoked NMDAR EPSCs. Traces were well fit with two exponentials, comprising fast and slow phases of decay and achieving an average R^2 fit of 0.9965 ± 0.0005 (n = 28 traces from 14 cells and 13 mice). We found no difference between the fast time constant (τ_f) of decay of control aCSF and ISO recordings, whether astrocytes were loaded with GDPβS or not (no GDPβS control aCSF 0.308 ± 0.031 s vs no GDPβS ISO 0.325 ± 0.028 s vs with GDPβS control aCSF 0.314 ± 0.043 s vs with GDPβS ISO 0.292 ± 0.017 s, Tukey-Kramer Post hoc, 2-Way ANOVA, n.s. between all groups $p > 0.88$) (Fig. 2H).

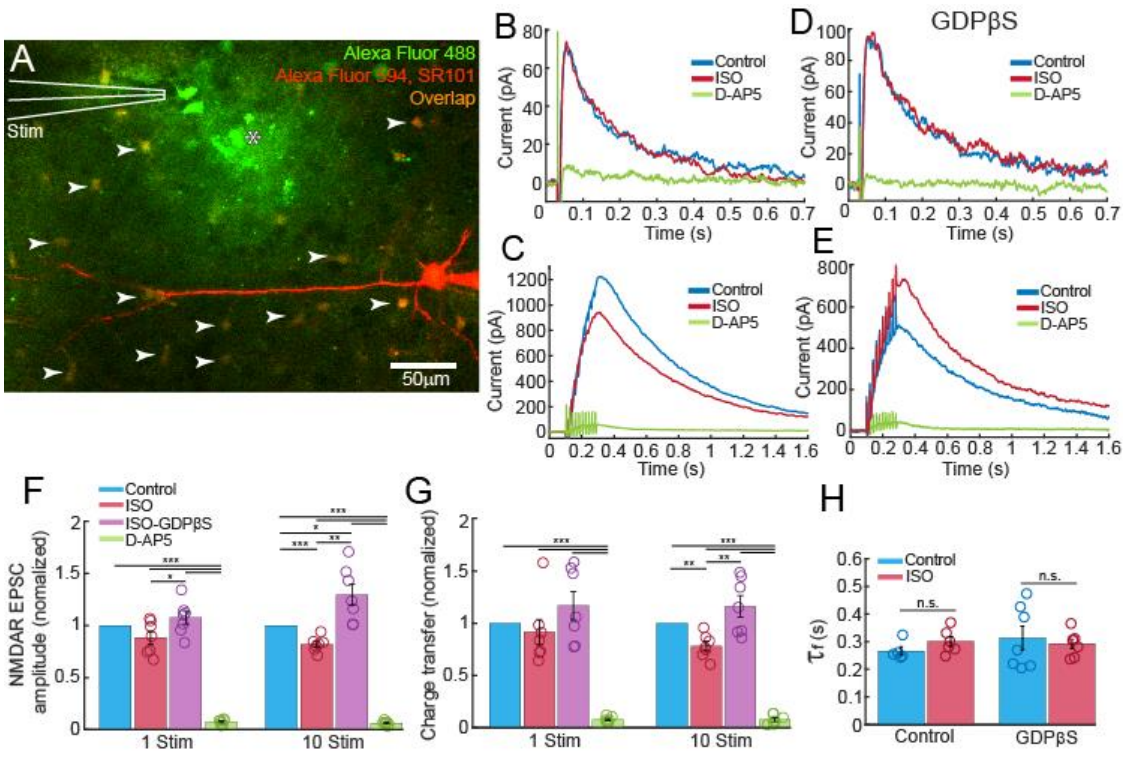

Figure 2. Ten stimuli-evoked NMDAR EPSCs are modulated by astrocyte β-AR activity. **A,** Confocal image of experimental arrangement for EPSC recording. A patched Layer 5 pyramidal neuron is filled with Alexa Fluor 594 (red) while astrocytes are initially labeled with SR 101 (also red). In some experiments, an astrocyte was patched (asterisk) and filled with GDPβS and Alexa Fluor 488 hydrazide (green), which diffused widely through the astrocyte network. SR 101-labeled astrocytes that are filled with GDPβS and Alexa Fluor 488 are orange (arrowheads) and surround the neuron. A theta tube pipette in Layer 2/3 (white lines, labeled Stim) evokes EPSCs in the labeled neuron. **B – E,** NMDAR EPSCs recorded from neurons in control aCSF (blue), after 40 min in ISO (red), and after an additional 5 min in D-AP5 (green). **B,** EPSCs evoked by single stimuli. **C,** EPSCs evoked by 10 stimuli bursts. **D,** EPSCs evoked by single stimuli with the astrocyte network loaded with GDPβS. **E,** EPSCs evoked by 10 stimuli bursts with the astrocyte network loaded with GDPβS. **F,** Summary of NMDAR EPSC amplitudes

(normalized to paired control aCSF EPSCs) elicited by single and 10 stimuli. Single stimulus groups include: control, all conditions, ISO (0.88 ± 0.06; n = 7 cells from 6 mice), ISO with GDPβS (1.07 ± 0.06; n = 7 cells from 7 mice), D-AP5 (0.08 ± 0.01; n = 7 cells from 5 mice). 10 stimuli groups include: control, all conditions, ISO (0.82 ± 0.03; n = 7 cells from 6 mice), ISO with GDPβS (1.30 ± 0.10; n = 7 cells from 7 mice), D-AP5 (0.06 ± 0.01; n = 7 cells from 5 mice). **G,** Summary of NMDAR EPSC charge transfer (normalized to paired control aCSF EPSCs) elicited by single and 10 stimuli. Single stimulus groups include: control, all conditions, ISO (0.91 ± 0.12; n = 7 cells from 6 mice), ISO with GDPβS (1.17 ± 0.13; n = 7 cells from 7 mice), D-AP5 (0.07 ± 0.01; n = 7 cells from 5 mice). 10 stimuli groups include: control, all conditions, ISO (0.78 ± 0.04; n = 7 cells from 6 mice), ISO with GDPβS (1.16 ± 0.10; n = 7 cells from 7 mice), D-AP5 (0.07 ± 0.02; n = 7 cells from 5 mice). In **F – G**, mean ± SEM and data from individual cells are shown; paired t-tests compare control and experimental groups, and D-AP5 to paired ISO trials. Comparisons between ISO with and without GDPβS use unpaired t-tests. *p < 0.05, **p < 0.01, ***p < 0.001. Exact p values contained within the text. **H,** Summary of the fast decay time constant (τ_f) from 10 stimuli-evoked NMDAR EPSCs. EPSC decay was fit by the sum of two exponentials (R^2 = 0.9965 ± 0.0005; n = 28 traces from 14 cells and 13 mice). Groups include: no GDPβS control (0.308 ± 0.031s; n = 7 cells from 6 mice), no GDPβS ISO (0.325 ± 0.028s; n = 7 cells from 6 mice), GDPβS control (0.314s ± 0.043s; n = 7 cells from 7 mice), GDPβS ISO (0.292s ± 0.017s; n = 7 cells from 7 mice). Mean ± SEM and data from individual cells are shown; 2-way ANOVA with Tukey-Kramer post hoc multiple comparisons, n.s. between all groups p > 0.88.

AMPA receptor currents are not affected by β-adrenergic receptor activation

Neurons express β-ARs and ISO could potentially act on presynaptic terminals as well as astrocytes, changing glutamate release (Ji et al., 2008). We measured AMPAR EPSCs with and without ISO and then with GDPβS-loaded astrocytes to determine whether changes in glutamate release could account for the changes we observed in NMDAR activity. Single stimulus AMPAR EPSCs recorded in ISO did not change significantly compared to control EPSCs, although they did trend larger (1.22 ± 0.13; n = 7 cells from 5 mice, paired t-test, n.s., p = 0.135) (Fig. 3A). Similarly, single stimulus AMPAR EPSCs in ISO with GDPβS-loaded astrocytes were not different from control EPSCs, although they did trend larger as well (1.28 ± 0.14, n = 7 cells from 6 mice, paired t-test, n.s., p = 0.09) (Fig. 3B). GDPβS did not impact the relative effect ISO had on AMPAR EPSCs (no GDPβS ISO vs GDPβS ISO; unpaired t-test, n.s., p = 0.729).

We also measured AMPAR EPSCs with the 10 stimulus paradigm to evaluate changes to overall synaptic facilitation or depression in the presence of ISO and GDPβS. The peak AMPAR EPSCs evoked by each of the 10 stimulus pulses were added together to reflect the overall synaptic glutamatergic activity: Σ AMPAR EPSCs (Fig. 3C, D). We observed that Σ AMPAR EPSCs trended larger with ISO compared to control EPSCs (1.25 ± 0.10, n = 7 cells from 5 mice, paired t-test, n.s., p = 0.0513) (Fig. 3C, E). Σ AMPAR EPSCs with GDPβS loaded astrocytes showed no difference between control and ISO recordings (1.05 ± 0.05, n = 7 cells from 6 mice, paired t-test, n.s., p = 0.391) (Fig. 3D, E). Further, the presence or absence of GDPβS did not affect the relative impact ISO had on Σ AMPAR EPSCs (no GDPβS ISO vs GDPβS ISO; unpaired t-test, n.s., p = 0.110). Figure 3E summarizes the results, showing that ISO and the presence of GDPβS had no significant effect on single or repetitive stimulus-evoked AMPAR

EPSCs. These results suggest that changes in glutamate release cannot account for the ISO-induced reduction in NMDAR currents in response to repetitive stimuli and are instead consistent with a role for β-AR-mediated astrocyte volume changes.

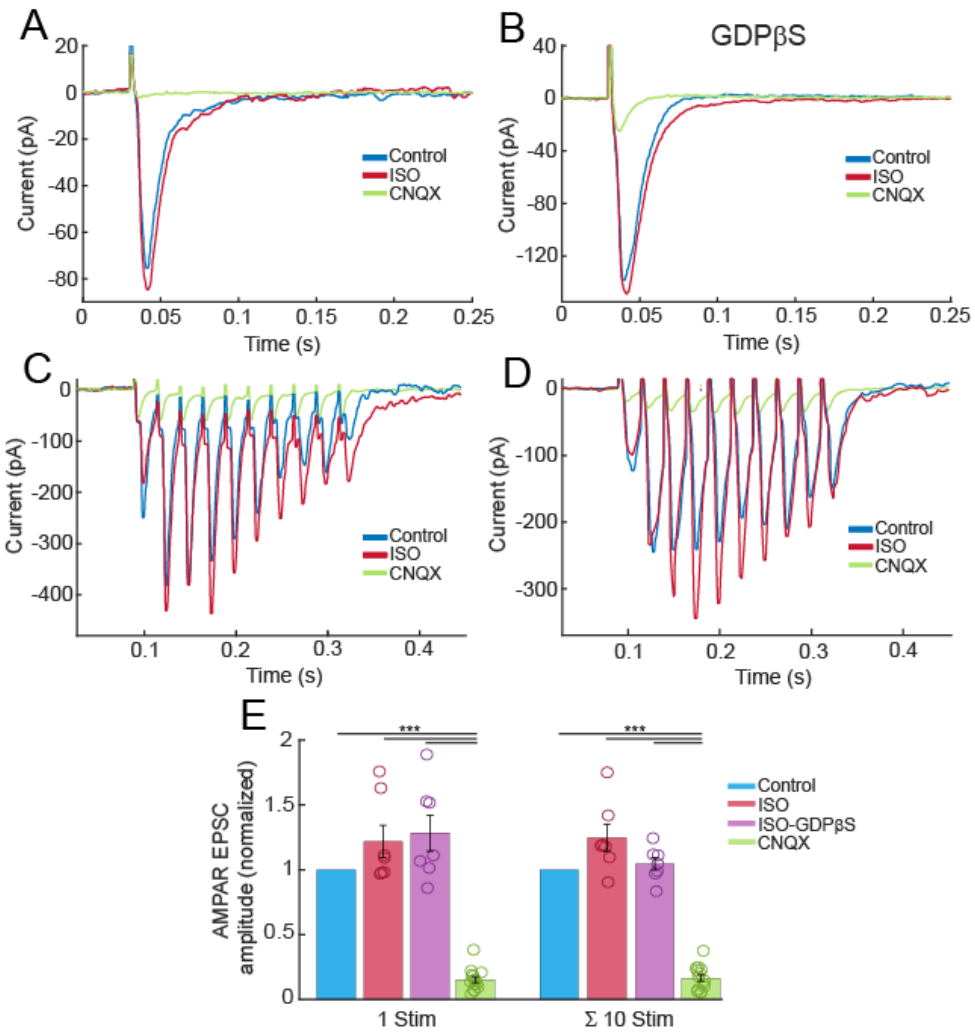

Figure 3. Single and 10 stimuli-evoked AMPAR EPSCs are not modulated by astrocyte β-AR activity. **A – D,** AMPAR EPSCs recorded from single neurons in control aCSF (blue), after 40 min in ISO (red), and after an additional 5 min in CNQX (green). **A,** EPSCs evoked by single stimuli. **B,** EPSCs evoked by single stimuli and the astrocyte network loaded with GDPβS. **C,** EPSCs evoked by 10 stimuli bursts. **D,** EPSCs evoked by 10 stimuli bursts and the astrocyte network loaded with GDPβS. **E,** Summary of single and 10 stimuli-evoked AMPAR EPSCs (normalized to paired controls). Mean ± SEM and data from individual cells are shown. Single stimulus groups include: control,

all conditions, ISO (1.22 ± 0.13; n = 7 cells from 5 mice), ISO with GDPβS (1.28 ± 0.14, n = 7 cells from 6 mice), CNQX (0.15 ± 0.02; n = 14 cells from 11 mice). 10 stimuli-evoked Σ AMPAR EPSC groups include: control, all conditions, ISO (1.25 ± 0.10, n = 7 cells from 5 mice), ISO with GDPβS (1.05 ± 0.05, n = 7 cells from 6 mice), CNQX (0.16 ± 0.03; n = 14 cells from 11 mice). Paired t-tests compare control and experimental groups, and comparisons between ISO groups with paired CNQX trials. ISO with and without GDPβS use unpaired t-tests. ***$p < 0.001$. Exact p values contained within the text.

β-adrenergic receptor signaling reduces extrasynaptic NMDAR currents

Delivering 10 stimuli at 50 Hz is sufficient to elicit glutamate spillover and activation of extrasynaptic NMDARs (Harris and Pettit, 2008). We sought to determine whether extrasynaptic NMDARs contributed to the currents reduced by ISO. MK-801 is an activity-dependent NMDAR blocker used to eliminate synaptic NMDARs activated by single pulse stimuli, leaving the unblocked extrasynaptic NMDARs to respond to a high-frequency repetitive stimulus (Harris and Pettit, 2008; Papouin et al., 2012; Yang et al., 2017). The process of isolating extrasynaptic NMDARs is illustrated in Figure 4A. After initial aCSF NMDAR EPSC recordings with single-pulse stimuli, neurons were incubated in MK-801 while delivering stimuli at 1 Hz. After 10 min, NMDAR EPSCs were reduced to near zero and the MK-801 was washed out. Stimulus delivery in MK-801 resulted in blocking single stimulus-evoked synaptic NMDAR currents, which was sustained throughout the rest of the recording session (Fig. 4B). The sustained blockade of single stimulus NMDAR EPSCs is summarized in Figure 4C. After a 15 min washout, post MK-801 control NMDAR EPSCs in aCSF were reduced by 88% (0.12 ± 0.01; n = 8 cells from 6 mice, paired t-test, *** $p = 9.62 \times 10^{-13}$). Synaptic NMDAR blockade was maintained through the 40 min ISO incubation as well and single stimulus NMDAR EPSCs in ISO were similar to post MK-801 control EPSCs (0.98 ± 0.01, n = 8 cells from 6 mice, pairwise t-test, n.s., p = 0.67) (Fig. 4B, C).

Maintained synaptic blockade allowed us to measure isolated extrasynaptic NMDAR currents in post MK-801 control aCSF and ISO conditions. Isolated extrasynaptic, repetitive stimuli-evoked NMDARs EPSCs were reduced in ISO to a similar degree as the NMDAR currents that were recorded when synaptic NMDARs were unblocked (Fig. 4D and Fig. 2E). As summarized by Figure 4E, 10 stimuli-evoked

extrasynaptic NMDAR EPSC amplitude was reduced by 16% in ISO compared to post MK-801 control aCSF (0.84 ± 0.02; n = 8 cells from 6 mice, paired t-test, ***p = 9.31 x 10^{-5}). NMDAR charge transfer was reduced by 8% (0.92 ± 0.03; n = 8 cells from 6 mice, paired t-test, *p = 0.039). These results suggest that β-AR activity reduces glutamate spillover from high-frequency repetitive stimulation and that limiting extrasynaptic NMDAR recruitment accounts, at least in part, for the reduced NMDAR EPSCs driven by astrocyte β-AR activation.

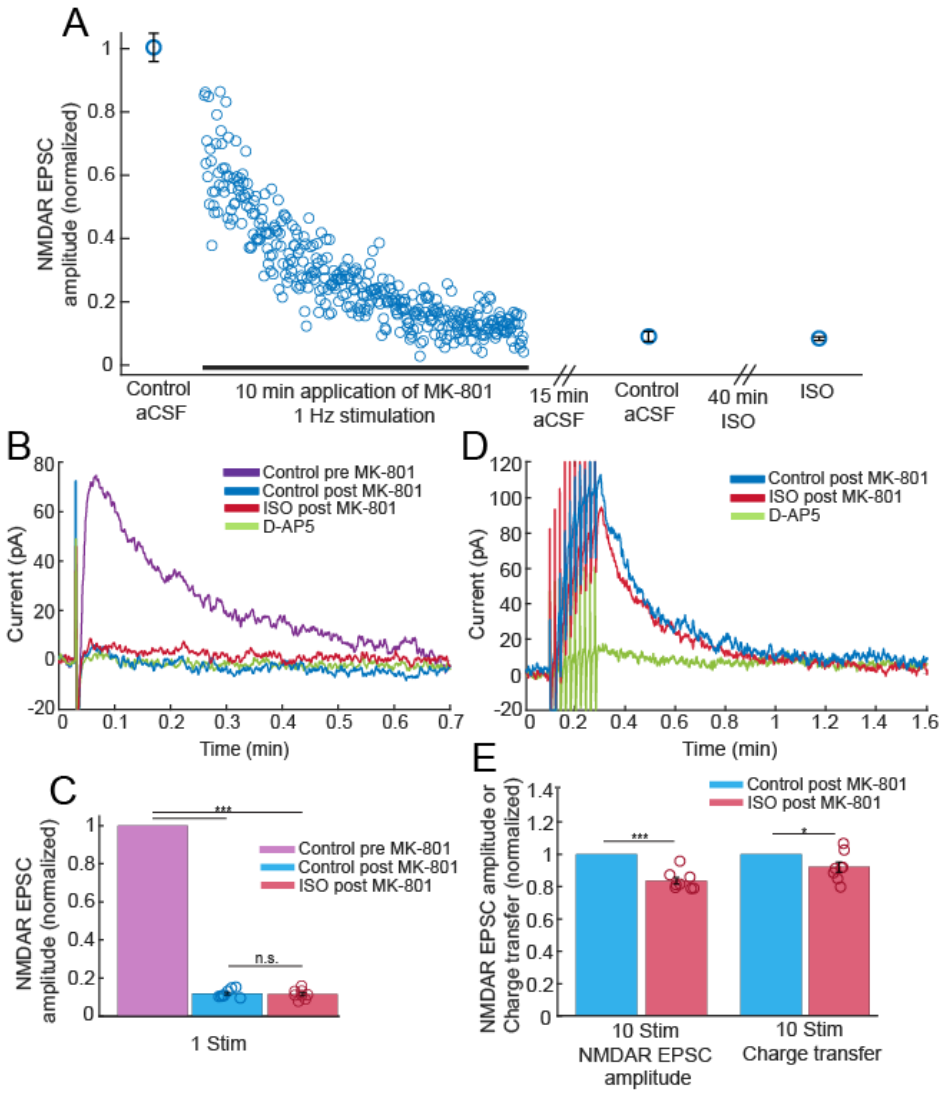

Figure 4. β-AR activity modulates extrasynaptic NMDAR EPSCs. **A,** Single stimulus-evoked NMDAR EPSCs tracking synaptic NMDAR blockade by MK-801, recorded from a single neuron (normalized to pre MK-801). Data points with error bars represent mean ± SEM. Data points during MK-801 treatment indicate individual EPSCs. Time course of 10 min MK-801 treatment is indicated by black bar. **B,** NMDAR EPSCs evoked by single stimuli, recorded from a single neuron. Pre MK-801 aCSF control (purple), post MK-801 aCSF (blue), post MK-801 after 40 min in ISO (red), and after an additional 5 min in D-AP5 (green). **C,** Summary of single stimulus NMDAR EPSCs (normalized to pre MK-801

control aCSF). Pre MK-801 control aCSF (purple), post MK-801 control aCSF (blue; 0.12 ± 0.01; n = 8 cells from 6 mice), ISO (red; 0.12 ± 0.01; n = 8 cells from 6 mice). Paired t-tests compare control pre and post MK-801 groups, as well as post MK-801 aCSF to post MK-801 ISO. n.s., $p > 0.05$, ***$p < 0.001$. **D,** NMDAR EPSCs evoked by 10 stimuli, recorded from a single neuron. Post MK-801 aCSF (blue), post MK 801 after 40 min in ISO (red) and after an additional 5 min in D-AP5 (green). **E,** Summary of 10 stimuli-evoked NMDAR EPSCs and charge transfer (normalized to post MK-801 control, blue). Post MK-801 ISO NMDAR EPSC amplitude (red, 0.84 ± 0.02; n = 8 cells from 6 mice) and post MK-801 ISO NMDAR EPSC charge transfer (red, 0.92 ± 0.03; n = 8 cells from 6 mice). Paired t-tests compare post MK-801 aCSF and post MK-801 ISO for NMDAR EPSC amplitude and charge transfer measures. *$p < 0.05$, ***$p < 0.001$. Mean ± SEM and data from individual cells are shown in C and E. Exact p values contained within the text.

Discussion

We have shown that astrocyte β-AR activity increases astrocyte process volume in the mPFC, limiting glutamate spillover and extrasynaptic NMDAR recruitment. We first measured changes to astrocyte process volume utilizing an established method of dye-filling astrocytes (Henneberger et al., 2020) and found that noradrenergic agonists increase astrocyte process volume by ~18% in the mPFC. This is in accord with prior studies which showed that astrocyte β-AR activity results in process expansion *in vitro* (Vardjan et al., 2014) as well as in the visual cortex (Sherpa et al., 2016), where treatment with ISO results in a 30% reduction in ECS volume fraction. Our work confirms that NE and β-ARs increase astrocyte volume in the mPFC, an unexplored area which is densely innervated by noradrenergic projections (Hoover and Vertes, 2007; Santana and Artigas, 2017). We also effectively blocked noradrenergic agonist-evoked increases to process volume by loading astrocytes with GDPβS. This agrees with findings from multiple studies which demonstrate that GDPβS loading of astrocytes blocks G-protein-mediated signaling from monoaminergic receptors (Navarrete et al., 2012; Corkrum et al., 2020).

We next demonstrated that β-AR activation reduces pyramidal neuron NMDAR currents in an astrocyte-dependent manner. In agreement with this finding, the reverse phenomenon has been reported in other systems: when decreases in astrocyte process volume are observed, enhanced glutamate spillover is seen (Oliet et al., 2004; Henneberger et al., 2020; Müller et al., 2021; Badia-Soteras et al., 2022). Our study found that NMDAR currents evoked by 10 stimuli bursts were reduced by ISO, consistent with the finding that increasing astrocyte process volume limits glutamate spillover (Popov et al., 2020).

The ISO effect could, in theory, be mediated by direct ISO activation of pyramidal neurons rather than by astrocytes, as these neurons also express β-ARs, which enhance neuronal EPSCs (Ji et al., 2008; Grzelka et al., 2017). However, we found that ISO did not affect single stimulus AMPAR or NMDAR currents. Furthermore, ISO reduced high-frequency repetitive stimulus-evoked NMDAR EPSCs instead of enhancing it. It was only after blocking astrocyte β-AR activity with GDPβS did ISO enhance repetitive stimulus-evoked NMDAR currents.

We then demonstrated that β-AR activity reduces extrasynaptic NMDAR recruitment. Several methods have previously been used to approximate or isolate extrasynaptic NMDAR activity. Prior work has shown that a 50 Hz repetitive stimulus overpowers glutamate uptake mechanisms, leading to glutamate spillover and the recruitment of extrasynaptic NMDARs (Harris and Pettit, 2008). Others have used the NMDAR activity-dependent blocker MK-801 to eliminate synaptic NMDAR currents through low frequency stimulation (Milnerwood et al., 2010; Liu et al., 2013; Yang et al., 2017; Pallas-Bazarra et al., 2019). In this work, we used both methods to study extrasynaptic NMDAR currents. Following MK-801 block of synaptic NMDAR currents, the residual extrasynaptic NMDAR current elicited by a 50 Hz repetitive stimulus was reduced by ISO to 84% of control. This decrease is similar to the ISO-induced reduction of the total NMDAR current evoked by 50 Hz repetitive stimulation (82%), suggesting that the ISO-mediated increase in astrocyte volume primarily reduces extrasynaptic NMDAR activation. These findings are consistent with prior work showing that increased astrocyte volume caused by caloric restriction results in decreased extrasynaptic NMDAR activity (Popov et al., 2020).

Although increased astrocyte volume reduces extrasynaptic NMDAR currents, questions regarding the specific mechanisms that contribute to volume change remain unanswered. Our method for quantifying astrocyte volume changes (Henneberger et al., 2020) did not allow us to determine the fine details of process volume changes or to differentiate between process expansion or swelling. ISO activation of β-ARs has been shown to elicit astrocyte process expansion and volume increases in primary astrocyte culture and in the rat visual cortex (Vardjan et al., 2014; Sherpa et al., 2016). β-AR activation is also linked to enhanced Na^+/K^+-ATPase activity and increased K^+ uptake into astrocytes, which is a mechanism associated with swelling (Walch et al., 2020; Wotton et al., 2020).

β-AR signaling acts on several astrocyte pathways that could affect NMDAR activity in addition to astrocyte volume changes. Previous work has shown that ISO modestly inhibits glutamate uptake in primary astrocyte cultures (Hansson and Rönnbäck, 1991, 1992). However, this would result in enhanced glutamate spillover and increased NMDAR signaling, the opposite of what we observed. Astrocyte β-AR activity also enhances glycogenolysis and lactate production, which has been shown to support LTP in the hippocampus and enhance EPSCs (Gao et al., 2016). This again runs counter to our observations that ISO reduces NMDAR activation. Astrocytes release gliotransmitters, including ATP and D-serine, that may influence glutamate release and NMDAR activity, respectively (Panatier et al., 2006; Henneberger et al., 2010; Chen et al., 2013). Norepinephrine has been shown to elicit astrocyte ATP release and increase AMPAR signaling (Gordon et al., 2005). Despite this possibility, in our experiments ISO had no significant effect on synaptic AMPAR or NMDAR single stimulus currents. However, single stimulus NMDAR EPSCs were significantly larger in ISO when

astrocytes were loaded with GDPβS compared to unloaded astrocytes. Since D-serine is a co-agonist for NMDARs, changes to D-serine secretion would impact NMDAR activity, although this has not been explored with ISO. Astrocytes can also release glutamate directly (Basarsky et al., 1999; Angulo et al., 2004; Woo et al., 2012). This would, however, result in an increase, not a decrease in extrasynaptic NMDAR activation.

Major depression in humans and depressive-like symptoms in animals are associated with impaired monoamine signaling, including NE (Ruhé et al., 2007; Moret and Briley, 2011). The effects of reduced NE signaling could be mediated by changes in astrocyte morphology. Indeed, retraction and a reduction of astrocyte process volume has been observed in suicide victims diagnosed with depression and mouse chronic stress models that produce depressive-like behavior (Torres-Platas et al., 2016; Codeluppi et al., 2021). Altered astrocyte morphology and process retraction have also been shown to impact neuronal circuits in emotion processing regions of the brain, enhancing fear memory (Badia-Soteras et al., 2022). Reduced astrocyte volume may impair the termination of synaptic glutamate signaling and result in spillover, enhancing extracellular glutamate and extrasynaptic NMDAR activation, which is seen in chronic stress models displaying depressive-like behavior (Li et al., 2018). Enhanced extrasynaptic NMDAR recruitment can also have harmful effects on neurons and on behavior (Hardingham et al., 2002; Milnerwood et al., 2010; Zhou et al., 2013; Hanson et al., 2015; Li et al., 2018), and the blockade of extrasynaptic NMDARs by new fast-acting antidepressants may contribute to depressive symptom relief (Miller et al., 2014; Li et al., 2018; Tang et al., 2020).

Our results are consistent with and support this mechanism of depression. Our observation that noradrenergic-mediated astrocyte volume increase leads to a reduction

in extrasynaptic NMDAR activity implies that the opposite is also true. That is, a reduction in noradrenergic activity would lead to astrocyte shrinkage and to an enhancement of extrasynaptic NMDAR activity.

Schizophrenia has been canonically linked to monoamine overactivation, including NE elevation (Breier, 1990; Nagamine, 2020). More recently, a NMDAR hypofunction hypothesis of schizophrenia has been proposed (Lahti et al., 1995; Uno and Coyle, 2019). The hypothesis holds that reduced levels of NMDAR activity contribute to schizophrenic symptoms. Overstimulation of astrocyte β-AR could result in excessive volume increases in these glial cells, limiting NMDAR activation.

Overall, our findings support previous research showing that astrocytes provide a crucial role in modulating neuronal activity and, specifically, glutamatergic signaling. Changes to astrocyte volume during various pathological conditions may well modulate extrasynaptic NMDAR activation. Uncovering novel mechanisms to modulate astrocyte volume changes will further elucidate how astrocyte morphology affects synaptic activity and animal behavior, possibly leading to new strategies for targeting neuropsychiatric disorders.

Chapter 3: Conclusion

Conclusions

These findings reaffirm the dynamic nature of astrocyte morphology and its impact on neuronal activity. We found β-AR activity increases astrocyte volume in a previously unexplored region of the brain: the mPFC. NE and β-AR agonist ISO acted directly through astrocyte β-ARs to increase process volume by ~18%, an effect blocked by eliminating G-protein signaling with GDPβS. Our findings demonstrate β-AR activity reduces neuronal NMDAR currents in an astrocyte-dependent manner. High frequency bursts of electric stimulus are associated with glutamate spillover and enhanced NMDAR recruitment. β-AR activation reduced the 10 stimuli-evoked NMDAR currents, in line with reports that increasing astrocyte volume reduces glutamate spillover. Likewise, we found ISO reduced extrasynaptic NMDAR recruitment, further evidence ISO limits spillover. Finally, blocking astrocyte β-AR signaling with GDPβS reversed the effect of ISO and led to ISO enhancing NMDAR currents evoked by 10 stimuli bursts. This research joins a growing list of studies demonstrating that astrocyte volume affects glutamate spillover and neuronal activity.

The mPFC is fundamental to execute function and emotion processing (Jason J. Radley et al., 2008; Santana and Artigas, 2017). When NE levels and extrasynaptic NMDAR activity are dysregulated in the mPFC, psychiatric disorders can symptoms follow (Breier, 1990; Ruhé et al., 2007; Szot et al., 2016; Li et al., 2018; Tang et al., 2020). For example, major depression is associated with NE hypoactivity and enhanced extrasynaptic NMDAR activity (Ruhé et al., 2007, Li et al., 2018). Furthermore, astrocyte volume is reduced in the brains of depressed individuals who committed suicide and mice that display depressive-like behavior (Rajkowska and Stockmeier, 2013; Codeluppi

et al., 2021). Our findings suggest that lower NE levels explain the reduced astrocyte volume, which then results in the enhanced extrasynaptic NMDAR activity associated with depressive-like behavior. Perhaps exploring new ways to specifically target and regulate astrocyte volume can help limit extrasynaptic NMDAR activity, opening the possibility to new anti-depressant treatments.

Future Directions

The findings of this thesis contribute to our understanding of the important role astrocyte physiology and morphology play in proper brain function and disease. This field is still growing and finding new ways to influence astrocyte morphology could someday reveal new ways astrocyte morphology interacts with neurons based on proximity. There are several questions that can clarify how β-AR activity modifies astrocyte morphology and ask how astrocyte morphology affects neuronal activity and behavior in the mPFC.

Are astrocyte process volume increases due to process remodeling or swelling? The mechanisms through which astrocyte process volume increases remain unclear. PKA and cAMP signaling have been shown to remodel astrocyte processes (Vardjan et al., 2014; Sherpa et al., 2016). Meanwhile, β-AR signaling enhances K^+ clearance through Na^+,K^+-ATPase activity, which has been associated with astrocyte swelling (Song et al., 2015; Wotton et al., 2020). Parsing out which mechanisms are at play could lead to more targeted means of manipulating astrocyte morphology.

Are there more specific ways to target and increase astrocyte process volume? Developing methods to exclusively target astrocytes to increase astrocyte process volume would provide a great tool to further assess and validate the role of astrocytes in

modulating neuronal NMDAR activity. Expressing Gs-GPCR designer receptors exclusively activated by designer drugs (DREADDs) in astrocytes could be one such way. Gs-DREADDs would exclusively increase cAMP in astrocytes to replicate β-AR signaling and, we would predict, increase astrocyte process volume. Beyond using Gs-DREADDs, which activate all cAMP pathways, finding means of specifically increasing astrocyte volume without interfering with other astrocyte functions would open a fascinating new field to measure how astrocyte volume and process proximity affects neuronal activity.

Can we visualize that glutamate spillover is limited by astrocyte β-AR activation and process volume increases? While we observed β-AR agonist ISO reduces extrasynaptic NMDAR recruitment, more could be done to verify reduced glutamate spillover. To observe how astrocyte volume changes influence glutamate spillover, one could visualize glutamate spillover using membrane-expressing glutamate optical sensors on astrocytes (Romanos et al., 2019). Based on our results, we would predict that ISO and manipulations to increase astrocyte process volume would limit glutamate diffusion and result in a faster decay of fluorescence signal.

Does increasing astrocyte process volume protect against or reverse depressive-like behavior? Astrocyte volume changes in various disease states. Chronic stress models reduce astrocyte process volume in the mPFC (Codeluppi et al., 2021). Future experiments could test whether increasing astrocyte volume alleviates and can provide resilience against depressive-like symptoms. Activating Gs-DREADDs expressed in astrocytes, if verified to increase astrocyte process volume, could provide an initial step towards evaluating how astrocyte process volume impacts depressive-like symptoms.

Finally, is mPFC ECS volume fraction larger in chronic stress models?

Decreased astrocyte process volume found in chronic stress models would imply that ECS volume fraction would be larger, but this has not been verified. Such changes could also explain the increased extracellular glutamate levels observed, and enhanced extrasynaptic NMDAR activity. Furthermore, future experiments could explore whether antidepressant drugs rescue both astrocyte volume and any changes to ECS volume fraction observed.

References

Acosta-Rodríguez V, Rijo-Ferreira F, Izumo M, Xu P, Wight-Carter M, Green CB, Takahashi JS (2022) Circadian alignment of early onset caloric restriction promotes longevity in male C57BL/6J mice. Science 376:1192–1202.

Aguado F, Espinosa-Parrilla JF, Carmona MA, Soriano E (2002) Neuronal activity regulates correlated network properties of spontaneous calcium transients in astrocytes *in situ*. J Neurosci 22:9430–9444.

Albrecht J, Wysmyk-Cybula U, Rafalowska U (1985) Na^+/K^+-ATPase activity and GABA uptake in astroglial cell-enriched fractions and synaptosomes derived from rats in the early stage of experimental hepatogenic encephalopathy. Acta Neurol Scand 72:317–320.

Alexandra M. Kaufman, Austen J. Milnerwood, Marja D. Sepers, Ainsley Coquinco, Kevin She, Liang Wang, Hwan Lee, Ann Marie Craig, Max Cynader, Lynn A. Raymond (2012) Opposing Roles of Synaptic and Extrasynaptic NMDA Receptor Signaling in Cocultured Striatal and Cortical Neurons. J Neurosci 32:3992.

Allam SL, Ghaderi VS, Bouteiller JM, Legendre A, Ambert N, Greget R, Bischoff S, Baudry M, Berger TW (2012) A computational model to investigate astrocytic glutamate uptake influence on synaptic transmission and neuronal spiking. Front Comput Neurosci 6:70.

Amundson RH, Goderie SK, Kimelberg HK (1992) Uptake of [^{3}H]serotonin and [^{3}H]glutamate by primary astrocyte cultures. II. Differences in cultures prepared from different brain regions. Glia 6:9–18.

Anderson CT, Radford RJ, Zastrow ML, Zhang DY, Apfel U-P, Lippard SJ, Tzounopoulos T (2015) Modulation of extrasynaptic NMDA receptors by synaptic and tonic zinc. Proc Natl Acad Sci 112:E2705–E2714.

Angulo MC, Kozlov AS, Charpak S, Audinat E (2004) Glutamate released from glial cells synchronizes neuronal activity in the hippocampus. J Neurosci 24:6920–6927.

Anna Cavaccini, Caitlin Durkee, Paulo Kofuji, Raffaella Tonini, Alfonso Araque (2020) Astrocyte Signaling Gates Long-Term Depression at Corticostriatal Synapses of the Direct Pathway. J Neurosci 40:5757.

Aoki C, Joh TH, Pickel VM (1987) Ultrastructural localization of beta-adrenergic receptor-like immunoreactivity in the cortex and neostriatum of rat brain. Brain Res 437:264–282.

Araque A, Parpura V, Sanzgiri RP, Haydon PG (1999a) Tripartite synapses: glia, the unacknowledged partner. Trends Neurosci 22:208–215.

Araque A, Sanzgiri RP, Parpura V, Haydon PG (1999b) Astrocyte-induced modulation of synaptic transmission. Can J Physiol Pharmacol 77:699–706.

Arizono M, Inavalli V, Panatier A, Pfeiffer T, Angibaud J, Levet F, Ter Veer MJT, Stobart J, Bellocchio L, Mikoshiba K, Marsicano G, Weber B, Oliet SHR, Nägerl UV (2020) Structural basis of astrocytic Ca(2+) signals at tripartite synapses. Nat Commun 11:1906.

Badia-Soteras A, Heistek TS, Kater MSJ, Mak A, Negrean A, Oever MC van den, Mansvelder HD, Khakh BS, Min R, Smit AB, Verheijen MHG (2022) Retraction of Astrocyte Leaflets From the Synapse Enhances Fear Memory. Biol Psychiatry 0 Available at: https://www.biologicalpsychiatryjournal.com/article/S0006-3223(22)01705-X/fulltext [Accessed April 25, 2023].

Basarsky TA, Feighan D, MacVicar BA (1999) Glutamate release through volume-activated channels during spreading depression. J Neurosci 19:6439–6445.

Baude A, Nusser Z, Roberts JDB, Mulvihill E, Jeffrey McIlhinney RA, Somogyi P (1993) The metabotropic glutamate receptor (mGluRIα) is concentrated at perisynaptic membrane of neuronal subpopulations as detected by immunogold reaction. Neuron 11:771–787.

Bay V, Butt AM (2012) Relationship between glial potassium regulation and axon excitability: a role for glial Kir4.1 channels. Glia 60:651–660.

Bazargani N, Attwell D (2016) Astrocyte calcium signaling: the third wave. Nat Neurosci 19:182–189.

Bazargani N, Attwell D (2017) Amines, Astrocytes, and Arousal. Neuron 94:228–231.

Bear MF (1996) A synaptic basis for memory storage in the cerebral cortex. Proc Natl Acad Sci U A 93:13453–13459.

Bekar LK, He W, Nedergaard M (2008) Locus coeruleus alpha-adrenergic-mediated activation of cortical astrocytes in vivo. Cereb Cortex 18:2789–2795.

Bekar LK, Wei HS, Nedergaard M (2012) The locus coeruleus-norepinephrine network optimizes coupling of cerebral blood volume with oxygen demand. J Cereb Blood Flow Metab 32:2135–2145.

Berger AJ, Dieudonné S, Ascher P (1998) Glycine Uptake Governs Glycine Site Occupancy at NMDA Receptors of Excitatory Synapses. J Neurophysiol 80:3336–3340.

Bergles DE, Jahr CE (1998) Glial contribution to glutamate uptake at Schaffer collateral-commissural synapses in the hippocampus. J Neurosci 18:7709–7716.

Bernardinelli Y, Salmon C, Jones EV, Farmer WT, Stellwagen D, Murai KK (2011) Astrocytes display complex and localized calcium responses to single-neuron stimulation in the hippocampus. J Neurosci 31:8905–8919.

Berridge CW, Waterhouse BD (2003) The locus coeruleus–noradrenergic system: modulation of behavioral state and state-dependent cognitive processes. Brain Res Rev 42:33–84.

Bezzi P, Carmignoto G, Pasti L, Vesce S, Rossi D, Lodi Rizzini B, Pozzan T, Volterra A (1998) Prostaglandins stimulate calcium-dependent glutamate release in astrocytes. Nature 391:281–285.

Bezzi P, Domercq M, Brambilla L, Galli R, Schols D, De Clercq E, Vescovi A, Bagetta G, Kollias G, Meldolesi J, Volterra A (2001) CXCR4-activated astrocyte glutamate release via TNFa: amplification by microglia triggers neurotoxicity. Nat Neurosci 4:702–710.

Biesecker KR, Srienc AI, Shimoda AM, Agarwal A, Bergles DE, Kofuji P, Newman EA (2016) Glial Cell Calcium Signaling Mediates Capillary Regulation of Blood Flow in the Retina. J Neurosci 36:9435–9445.

Binder DK, Papadopoulos MC, Haggie PM, Verkman AS (2004) *In vivo* measurement of brain extracellular space diffusion by cortical surface photobleaching. J Neurosci 24:8049–8056.

Bindocci E, Savtchouk I, Liaudet N, Becker D, Carriero G, Volterra A (2017) Three-dimensional Ca(2+) imaging advances understanding of astrocyte biology. Science 356.

Boison D (2012) Adenosine dysfunction in epilepsy. Glia 60:1234–1243.

Boulay A-C, Saubaméa B, Adam N, Chasseigneaux S, Mazaré N, Gilbert A, Bahin M, Bastianelli L, Blugeon C, Perrin S, Pouch J, Ducos B, Le Crom S, Genovesio A, Chrétien F, Declèves X, Laplanche J-L, Cohen-Salmon M (2017) Translation in astrocyte distal processes sets molecular heterogeneity at the gliovascular interface. Cell Discov 3:17005.

Breier A (1990) Plasma norepinephrine in chronic schizophrenia. Am J Psychiatry 147:1467–1470.

Bushong EA, Martone ME, Jones YZ, Ellisman MH (2002) Protoplasmic astrocytes in CA1 stratum radiatum occupy separate anatomical domains. J Neurosci 22:183–192.

Cavalcante LA, Garcia-Abreu J, Moura Neto V, Silva LC, Barradas PC (1996) Heterogeneity of median and lateral midbrain radial glia and astrocytes. Rev Bras Biol 56 Su 1 Pt 1:33–52.

Chalermpalanupap T, Schroeder JP, Rorabaugh JM, Liles LC, Lah JJ, Levey AI, Weinshenker D (2018) Locus Coeruleus Ablation Exacerbates Cognitive Deficits, Neuropathology, and Lethality in P301S Tau Transgenic Mice. J Neurosci 38:74–92.

Chalifoux JR, Carter AG (2011) Glutamate spillover promotes the generation of NMDA spikes. J Neurosci 31:16435–16446.

Chandley MJ, Szebeni K, Szebeni A, Crawford J, Stockmeier CA, Turecki G, Miguel-Hidalgo JJ, Ordway GA (2013) Gene expression deficits in pontine locus coeruleus astrocytes in men with major depressive disorder. J Psychiatry Neurosci 38:276–284.

Chen J, Tan Z, Zeng L, Zhang X, He Y, Gao W, Wu X, Li Y, Bu B, Wang W, Duan S (2013) Heterosynaptic long-term depression mediated by ATP released from astrocytes. Glia 61:178–191.

Chen S, Diamond JS (2002) Synaptically released glutamate activates extrasynaptic NMDA receptors on cells in the ganglion cell layer of rat retina. J Neurosci 22:2165–2173.

Chever O, Djukic B, McCarthy KD, Amzica F (2010) Implication of Kir4.1 channel in excess potassium clearance: an in vivo study on anesthetized glial-conditional Kir4.1 knock-out mice. J Neurosci 30:15769–15777.

Chiang P-P, Kuo SP, Newman EA (2022) Cellular mechanisms mediating activity-dependent extracellular space shrinkage in the retina. Glia 70:1927–1937.

Chiu AM, Wang J, Fiske MP, Hubalkova P, Barse L, Gray JA, Sanz-Clemente A (2019) NMDAR-Activated PP1 Dephosphorylates GluN2B to Modulate NMDAR Synaptic Content. Cell Rep 28:332-341 e5.

Codeluppi SA, Chatterjee D, Prevot TD, Bansal Y, Misquitta KA, Sibille E, Banasr M (2021) Chronic Stress Alters Astrocyte Morphology in Mouse Prefrontal Cortex. Int J Neuropsychopharmacol 24:842–853.

Colbourn R, Hrabe J, Nicholson C, Perkins M, Goodman JH, Hrabetova S (2021) Rapid volume pulsation of the extracellular space coincides with epileptiform activity in mice and depends on the NBCe1 transporter. J Physiol 599:3195–3220.

Collingridge GL, Singer W (1990) Excitatory amino acid receptors and synaptic plasticity. Trends Pharmacol Sci 11:290–296.

Cooper JM, Halter KA, Prosser RA (2018) Circadian rhythm and sleep-wake systems share the dynamic extracellular synaptic milieu. Neurobiol Sleep Circadian Rhythms 5:15–36.

Corkrum M, Covelo A, Lines J, Bellocchio L, Pisansky M, Loke K, Quintana R, Rothwell PE, Lujan R, Marsicano G, Martin ED, Thomas MJ, Kofuji P, Araque A (2020) Dopamine-Evoked Synaptic Regulation in the Nucleus Accumbens Requires Astrocyte Activity. Neuron 105:1036-1047.e5.

Cornell-Bell AH, Finkbeiner SM, Cooper MS, Smith SJ (1990) Glutamate induces calcium waves in cultured astrocytes: long-range glial signaling. Science 247:470–473.

Coulter DA, Eid T (2012) Astrocytic regulation of glutamate homeostasis in epilepsy. Glia 60:1215–1226.

Covelo A, Araque A (2018) Neuronal activity determines distinct gliotransmitter release from a single astrocyte. Elife 7.

D'Ascenzo M, Fellin T, Terunuma M, Revilla-Sanchez R, Meaney DF, Auberson YP, Moss SJ, Haydon PG (2007) mGluR5 stimulates gliotransmission in the nucleus accumbens. Proc Natl Acad Sci U A 104:1995–2000.

De Pittà M, Goldberg M, Volman V, Berry H, Ben-Jacob E (2009) Glutamate regulation of calcium and IP_3 oscillating and pulsating dynamics in astrocytes. J Biol Phys 35:383–411.

Del Franco AP, Chiang P-P, Newman EA (2022) Dilation of cortical capillaries is not related to astrocyte calcium signaling. Glia 70:508–521.

Delgado JY, Fink AE, Grant SGN, O'Dell TJ, Opazo P (2018) Rapid homeostatic downregulation of LTP by extrasynaptic GluN2B receptors. J Neurophysiol 120:2351–2357.

Dembrow N, Johnston D (2014) Subcircuit-specific neuromodulation in the prefrontal cortex. Front Neural Circuits 8:54.

Di Castro MA, Chuquet J, Liaudet N, Bhaukaurally K, Santello M, Bouvier D, Tiret P, Volterra A (2011) Local Ca^{2+} detection and modulation of synaptic release by astrocytes. Nat Neurosci 14:1276–1284.

Diamond JS (2005) Deriving the glutamate clearance time course from transporter currents in CA1 hippocampal astrocytes: transmitter uptake gets faster during development. J Neurosci 25:2906–2916.

Ding F, O'Donnell J, Xu Q, Kang N, Goldman N, Nedergaard M (2016) Changes in the composition of brain interstitial ions control the sleep-wake cycle. Science 352:550–555.

Domingos C, Müller FE, Passlick S, Wachten D, Ponimaskin E, Schwarz MK, Schoch S, Zeug A, Henneberger C (2023) Induced Remodelling of Astrocytes In Vitro and In Vivo by Manipulation of Astrocytic RhoA Activity. Cells 12.

Duffy S, Macvicar BA (1995) Adrenergic Calcium Signaling in Astrocyte Networks within the Hippocampal Slice. J Neurosci 15:5535–5550.

Dunn KM, Hill-Eubanks DC, Liedtke WB, Nelson MT (2013) TRPV4 channels stimulate Ca^{2+}-induced Ca^{2+} release in astrocytic endfeet and amplify neurovascular coupling responses. Proc Natl Acad Sci U A 110:6157–6162.

Dupuis JP, Ladépêche L, Seth H, Bard L, Varela J, Mikasova L, Bouchet D, Rogemond V, Honnorat J, Hanse E, Groc L (2014) Surface dynamics of GluN2B-NMDA

receptors controls plasticity of maturing glutamate synapses. EMBO J 33:842–861.

Durán E, Pandinelli M, Logothetis NK, Eschenko O (2023) Altered norepinephrine transmission after spatial learning impairs sleep-mediated memory consolidation in rats. Sci Rep 13:4231.

Eduardo E. Benarroch (2009) The locus ceruleus norepinephrine system. Neurology 73:1699.

Fernandez AM, Martinez-Rachadell L, Navarrete M, Pose-Utrilla J, Davila JC, Pignatelli J, Diaz-Pacheco S, Guerra-Cantera S, Viedma-Moreno E, Palenzuela R, Ruiz de Martin Esteban S, Mostany R, Garcia-Caceres C, Tschöp M, Iglesias T, de Ceballos ML, Gutierrez A, Torres Aleman I (2022) Insulin regulates neurovascular coupling through astrocytes. Proc Natl Acad Sci 119:e2204527119.

Flint AC, Maisch US, Weishaupt JH, Kriegstein AR, Monyer H (1997) NR2A subunit expression shortens NMDA receptor synaptic currents in developing neocortex. J Neurosci 17:2469–2476.

Florence CM, Baillie LD, Mulligan SJ (2012) Dynamic Volume Changes in Astrocytes Are an Intrinsic Phenomenon Mediated by Bicarbonate Ion Flux. PLoS ONE 7:e51124.

Frances Davies M, Tsui J, Flannery JA, Li X, DeLorey TM, Hoffman BB (2004) Activation of α2 Adrenergic Receptors Suppresses Fear Conditioning: Expression of c-Fos and Phosphorylated CREB in Mouse Amygdala. Neuropsychopharmacology 29:229–239.

Gao V, Suzuki A, Magistretti PJ, Lengacher S, Pollonini G, Steinman MQ, Alberini CM (2016) Astrocytic β2-adrenergic receptors mediate hippocampal long-term memory consolidation. Proc Natl Acad Sci U S A 113:8526–8531.

Genoud C, Quairiaux C, Steiner P, Hirling H, Welker E, Knott GW (2006) Plasticity of astrocytic coverage and glutamate transporter expression in adult mouse cortex. PLoS Biol 4:e343.

Giaume C, Marin P, Cordier J, Glowinski J, Premont J (1991) Adrenergic regulation of intercellular communications between cultured striatal astrocytes from the mouse. Proc Natl Acad Sci U A 88:5577–5581.

Gordon GR, Baimoukhametova DV, Hewitt SA, Rajapaksha WR, Fisher TE, Bains JS (2005) Norepinephrine triggers release of glial ATP to increase postsynaptic efficacy. Nat Neurosci 8:1078–1086.

Gottesman II, Shields J (1967) A polygenic theory of schizophrenia. Proc Natl Acad Sci U A 58:199–205.

Gray SR, Ye L, Ye JY, Paukert M (2021) Noradrenergic terminal short-term potentiation enables modality-selective integration of sensory input and vigilance state. Sci Adv 7:eabk1378.

Grzelka K, Kurowski P, Gawlak M, Szulczyk P (2017) Noradrenaline Modulates the Membrane Potential and Holding Current of Medial Prefrontal Cortex Pyramidal Neurons via β1-Adrenergic Receptors and HCN Channels. Front Cell Neurosci 11 Available at: https://www.frontiersin.org/articles/10.3389/fncel.2017.00341.

Habbas S, Santello M, Becker D, Stubbe H, Zappia G, Liaudet N, Klaus FR, Kollias G, Fontana A, Pryce CR, Suter T, Volterra A (2015) Neuroinflammatory TNFa Impairs Memory via Astrocyte Signaling. Cell 163:1730–1741.

Haj-Yasein NN, Jensen V, Østby I, Omholt SW, Voipio J, Kaila K, Ottersen OP, Hvalby Ø, Nagelhus EA (2012) Aquaporin-4 regulates extracellular space volume dynamics during high-frequency synaptic stimulation: a gene deletion study in mouse hippocampus. Glia 60:867–874.

Halassa MM, Fellin T, Haydon PG (2007a) The tripartite synapse: roles for gliotransmission in health and disease. Trends Mol Med 13:54–63.

Halassa MM, Fellin T, Takano H, Dong JH, Haydon PG (2007b) Synaptic islands defined by the territory of a single astrocyte. J Neurosci 27:6473–6477.

Hanson JE, Pare J-F, Deng L, Smith Y, Zhou Q (2015) Altered GluN2B NMDA receptor function and synaptic plasticity during early pathology in the PS2APP mouse model of Alzheimer's disease. Neurobiol Dis 74:254–262.

Hansson E, Rönnbäck L (1991) Receptor regulation of the glutamate, GABA and taurine high-affinity uptake into astrocytes in primary culture. Brain Res 548:215–221.

Hansson E, Rönnbäck L (1992) Adrenergic receptor regulation of amino acid neurotransmitter uptake in astrocytes. Brain Res Bull 29:297–301.

Harada T, Harada C, Watanabe M, Inoue Y, Sakagawa T, Nakayama N, Sasaki S, Okuyama S, Watase K, Wada K, Tanaka K (1998) Functions of the two glutamate transporters GLAST and GLT-1 in the retina. Proc Natl Acad Sci U A 95:4663–4666.

Hardingham GE, Bading H (2010) Synaptic versus extrasynaptic NMDA receptor signalling: implications for neurodegenerative disorders. Nat Rev Neurosci 11:682–696.

Hardingham GE, Fukunaga Y, Bading H (2002) Extrasynaptic NMDARs oppose synaptic NMDARs by triggering CREB shut-off and cell death pathways. Nat Neurosci 5:405–414.

Harris AZ, Pettit DL (2008) Recruiting extrasynaptic NMDA receptors augments synaptic signaling. J Neurophysiol 99:524–533.

Heidbreder CA, Groenewegen HJ (2003) The medial prefrontal cortex in the rat: evidence for a dorso-ventral distinction based upon functional and anatomical characteristics. Neurosci Biobehav Rev 27:555–579.

Heller JP, Odii T, Zheng K, Rusakov DA (2019) Imaging tripartite synapses using super-resolution microscopy. Methods.

Henneberger C et al. (2020) LTP Induction Boosts Glutamate Spillover by Driving Withdrawal of Perisynaptic Astroglia. Neuron 108:919-936.e11.

Henneberger C, Papouin T, Oliet SHR, Rusakov DA (2010) Long-term potentiation depends on release of d-serine from astrocytes. Nature 463:232–236.

Henneberger C, Rusakov DA (2012) Monitoring local synaptic activity with astrocytic patch pipettes. Nat Protoc 7:2171–2179.

Herde MK, Bohmbach K, Domingos C, Vana N, Komorowska-Müller JA, Passlick S, Schwarz I, Jackson CJ, Dietrich D, Schwarz MK, Henneberger C (2020) Local Efficacy of Glutamate Uptake Decreases with Synapse Size. Cell Rep 32:108182.

Hertz L, Chen Y (2016) Importance of astrocytes for potassium ion (K(+)) homeostasis in brain and glial effects of K(+) and its transporters on learning. Neurosci Biobehav Rev 71:484–505.

Hertz L, Lovatt D, Goldman SA, Nedergaard M (2010) Adrenoceptors in brain: Cellular gene expression and effects on astrocytic metabolism and [Ca2+]i. Glia Neurotransmitter Sources Sens 57:411–420.

Hirase H, Iwai Y, Takata N, Shinohara Y, Mishima T (2014) Volume transmission signalling via astrocytes. Philos Trans R Soc Lond B Biol Sci 369:20130604.

Hirase H, Qian L, Bartho P, Buzsaki G (2004) Calcium dynamics of cortical astrocytic networks *in vivo*. PLoS Biol 2:E96.

Hires SA, Zhu Y, Tsien RY (2008) Optical measurement of synaptic glutamate spillover and reuptake by linker optimized glutamate-sensitive fluorescent reporters. Proc Natl Acad Sci U A 105:4411–4416.

Hoover WB, Vertes RP (2007) Anatomical analysis of afferent projections to the medial prefrontal cortex in the rat. Brain Struct Funct 212:149–179.

Hösli L, Binini N, Ferrari KD, Thieren L, Looser ZJ, Zuend M, Zanker HS, Berry S, Holub M, Möbius W, Ruhwedel T, Nave K-A, Giaume C, Weber B, Saab AS (2022) Decoupling astrocytes in adult mice impairs synaptic plasticity and spatial learning. Cell Rep 38:110484.

Houades V, Koulakoff A, Ezan P, Seif I, Giaume C (2008) Gap junction-mediated astrocytic networks in the mouse barrel cortex. J Neurosci 28:5207–5217.

Huang H, Bordey A (2004) Glial glutamate transporters limit spillover activation of presynaptic NMDA receptors and influence synaptic inhibition of Purkinje neurons. J Neurosci 24:5659–5669.

Huang R, Shuaib A, Hertz L (1993) Glutamate uptake and glutamate content in primary cultures of mouse astrocytes during anoxia, substrate deprivation and simulated

ischemia under normothermic and hypothermic conditions. Brain Res 618:346–351.

Huettner JE, Bean BP (1988) Block of N-methyl-D-aspartate-activated current by the anticonvulsant MK-801: selective binding to open channels. Proc Natl Acad Sci U A 85:1307–1311.

Inazu M, Takeda H, Matsumiya T (2003) Functional expression of the norepinephrine transporter in cultured rat astrocytes. J Neurochem 84:136–144.

Israel JM, Schipke CG, Ohlemeyer C, Theodosis DT, Kettenmann H (2003) $GABA_A$ receptor-expressing astrocytes in the supraoptic nucleus lack glutamate uptake and receptor currents. Glia 44:102–110.

Ivanov A, Pellegrino C, Rama S, Dumalska I, Salyha Y, Ben-Ari Y, Medina I (2006) Opposing role of synaptic and extrasynaptic NMDA receptors in regulation of the extracellular signal-regulated kinases (ERK) activity in cultured rat hippocampal neurons. J Physiol 572:789–798.

Jason J. Radley, Brandon Williams, Paul E. Sawchenko (2008) Noradrenergic Innervation of the Dorsal Medial Prefrontal Cortex Modulates Hypothalamo-Pituitary-Adrenal Responses to Acute Emotional Stress. J Neurosci 28:5806.

Ji X-H, Cao X-H, Zhang C-L, Feng Z-J, Zhang X-H, Ma L, Li B-M (2008) Pre- and Postsynaptic β-Adrenergic Activation Enhances Excitatory Synaptic Transmission in Layer V/VI Pyramidal Neurons of the Medial Prefrontal Cortex of Rats. Cereb Cortex 18:1506–1520.

Jo AO, Ryskamp DA, Phuong TTT, Verkman AS, Yarishkin O, MacAulay N, Križaj D (2015) TRPV4 and AQP4 Channels Synergistically Regulate Cell Volume and Calcium Homeostasis in Retinal Müller Glia. J Neurosci 35:13525–13537.

John CS, Smith KL, Van'T Veer A, Gompf HS, Carlezon WA, Cohen BM, Öngür D, Bechtholt-Gompf AJ (2012) Blockade of Astrocytic Glutamate Uptake in the Prefrontal Cortex Induces Anhedonia. Neuropsychopharmacology 37:2467–2475.

Johnson KM, Milner R, Crocker SJ (2015) Extracellular matrix composition determines astrocyte responses to mechanical and inflammatory stimuli. Neurosci Lett 600:104–109.

Joseph DP, Miller SS (1988) Alpha-adrenergic receptors mediate basal membrane voltage and resistance changes in bovine retinal pigment epithelium (RPE). Invest Ophthalmol Vis Sci Suppl. 29:20.

Jung JS, Bhat RV, Preston GM, Guggino WB, Baraban JM (1994) Molecular characterization of an aquaporin cDNA from brain: Candidate osmoregulator of water balance. Proc Natl Acad Sci U A 91:13052–13056.

Kalinin S, Gavrilyuk V, Polak PE, Vasser R, Zhao J, Heneka MT, Feinstein DL (2007) Noradrenaline deficiency in brain increases β-amyloid plaque burden in an animal model of Alzheimer's disease. Neurobiol Aging 28:1206–1214.

Kettenmann H, Ransom BR (1988) Electrical coupling between astrocytes and between oligodendrocytes studied in mammalian cell cultures. Glia 1:64–73.

Khakh BS, McCarthy KD (2015) Astrocyte Calcium Signaling: From Observations to Functions and the Challenges Therein. Cold Spring Harb Perspect Biol 7:a020404.

Kim R, Sepulveda-Orengo MT, Healey KL, Williams EA, Reissner KJ (2018) Regulation of Glutamate Transporter 1 (GLT-1) Gene Expression by Cocaine Self-Administration and Withdrawal. Neuropharmacology 128:1–10.

Kimelberg HK, Rutledge E, Goderie S, Charniga C (1995) Astrocytic swelling due to hypotonic or high K^+ medium causes inhibition of glutamate and aspartate uptake and increases their release. J Cereb Blood Flow Metab 15:409–416.

Kinney JP, Spacek J, Bartol TM, Bajaj CL, Harris KM, Sejnowski TJ (2013) Extracellular Sheets and Tunnels Modulate Glutamate Diffusion in Hippocampal Neuropil. J Comp Neurol 521:448–464.

Kirischuk S, Tuschick S, Verkhratsky A, Kettenmann H (1996) Calcium signalling in mouse Bergmann glial cells mediated by alpha1-adrenoreceptors and H1 histamine receptors. Eur J Neurosci 8:1198–1208.

Kiss JP, Szasz BK, Fodor L, Mike A, Lenkey N, Kurkó D, Nagy J, Vizi ES (2012) GluN2B-containing NMDA receptors as possible targets for the neuroprotective and antidepressant effects of fluoxetine. Neurochem Int 60:170–176.

Kitayama IT, Otani M, Murase S (2008) Degeneration of the Locus Ceruleus Noradrenergic Neurons in the Stress-induced Depression of Rats. Ann N Y Acad Sci 1148:95–98.

Klatte K, Kirschstein T, Otte D, Pothmann L, Müller L, Tokay T, Kober M, Uebachs M, Zimmer A, Beck H (2013) Impaired D-serine-mediated cotransmission mediates cognitive dysfunction in epilepsy. J Neurosci 33:13066–13080.

Kucheryavykh YV, Kucheryavykh LY, Nichols CG, Maldonado HM, Baksi K, Reichenbach A, Skatchkov SN, Eaton MJ (2007) Downregulation of Kir4.1 inward rectifying potassium channel subunits by RNAi impairs potassium transfer and glutamate uptake by cultured cortical astrocytes. Glia 55:274–281.

Kucukdereli H, Allen NJ, Lee AT, Feng A, Ozlu MI, Conatser LM, Chakraborty C, Workman G, Weaver M, Sage EH, Barres BA, Eroglu C (2011) Control of

excitatory CNS synaptogenesis by astrocyte-secreted proteins Hevin and SPARC. Proc Natl Acad Sci 108:E440–E449.

Kuo SP, Chiang P-P, Nippert AR, Newman EA (2020) Spatial Organization and Dynamics of the Extracellular Space in the Mouse Retina. J Neurosci:JN-RM-1717-20.

Kuroda M, Yokofujita J, Murakami K (1998) An ultrastructural study of the neural circuit between the prefrontal cortex and the mediodorsal nucleus of the thalamus. Prog Neurobiol 54:417–458.

Lahti AC, Holcomb HH, Medoff DR, Tamminga CA (1995) Ketamine activates psychosis and alters limbic blood flow in schizophrenia. NeuroReport 6 Available at: https://journals.lww.com/neuroreport/Fulltext/1995/04190/Ketamine_activates_psychosis_and_alters_limbic.11.aspx.

Larsen BR, Assentoft M, Cotrina ML, Hua SZ, Nedergaard M, Kaila K, Voipio J, MacAulay N (2014) Contributions of the Na+/K+-ATPase, NKCC1, and Kir4.1 to hippocampal K+ clearance and volume responses. Glia 62:608–622.

Larsen BR, MacAulay N (2017) Activity-dependent astrocyte swelling is mediated by pH-regulating mechanisms. Glia 65:1668–1681.

Larsen BR, Stoica A, MacAulay N (2019) Developmental maturation of activity-induced K(+) and pH transients and the associated extracellular space dynamics in the rat hippocampus. J Physiol 597:583–597.

Laureys G, Clinckers R, Gerlo S, Spooren A, Wilczak N, Kooijman R, Smolders I, Michotte Y, De Keyser J (2010) Astrocytic β2-adrenergic receptors: From physiology to pathology. Prog Neurobiol 91:189–199.

Lehmenkuhler A, Sykova E, Svoboda J, Zilles K, Nicholson C (1993) Extracellular-Space Parameters in the Rat Neocortex and Subcortical White-Matter during Postnatal-Development Determined by Diffusion Analysis. Neuroscience 55:339–351.

Lerea LS, McCarthy KD (1989) Astroglial cells in vitro are heterogeneous with respect to expression of the a_1-adrenergic receptor. Glia 2:135–147.

Li C, Tang Y, Li F, Turner S, Li K, Zhou X, Centola M, Yan X, Cao W (2006) 17beta-estradiol (bE_2) protects human retinal Muller cell against oxidative stress in vitro: evaluation of its effects on gene expression by cDNA microarray. Glia 53:392–400.

Li SX, Han Y, Xu LZ, Yuan K, Zhang RX, Sun CY, Xu DF, Yuan M, Deng JH, Meng SQ, Gao XJ, Wen Q, Liu LJ, Zhu WL, Xue YX, Zhao M, Shi J, Lu L (2018) Uncoupling DAPK1 from NMDA receptor GluN2B subunit exerts rapid antidepressant-like effects. Mol Psychiatry 23:597–608.

Lisjak M, Potokar M, Rituper B, Jorgacevski J, Zorec R (2017) AQP4e-Based Orthogonal Arrays Regulate Rapid Cell Volume Changes in Astrocytes. J Neurosci 37:10748–10756.

Liu D, Yang Q, Li S (2013) Activation of extrasynaptic NMDA receptors induces LTD in rat hippocampal CA1 neurons. Extrasynaptic Ionotropic Recept 93:10–16.

Lydie Morel, Ming Sum R. Chiang, Haruki Higashimori, Temitope Shoneye, Lakshmanan K. Iyer, Julia Yelick, Albert Tai, Yongjie Yang (2017) Molecular and Functional Properties of Regional Astrocytes in the Adult Brain. J Neurosci 37:8706.

Ma Z, Stork T, Bergles DE, Freeman MR (2016) Neuromodulators signal through astrocytes to alter neural circuit activity and behaviour. Nature.

MacVicar BA, Tse FWY, Crichton SA, Kettenmann H (1989) GABA-activated Cl^- channels in astrocytes of hippocampal slices. J Neurosci 9:3577–3583.

Maity S, Rah S, Sonenberg N, Gkogkas CG, Nguyen PV (2015) Norepinephrine triggers metaplasticity of LTP by increasing translation of specific mRNAs. Learn Mem 22:499–508.

Manning TJ, Rosenfeld SS, Sontheimer H (1998) Lysophosphatidic acid stimulates actomyosin contraction in astrocytes. J Neurosci Res 53:343–352.

Martineau M, Galli T, Baux G, Mothet JP (2008) Confocal imaging and tracking of the exocytotic routes for D-serine-mediated gliotransmission. Glia 56:1271–1284.

Marvin JS, Borghuis BG, Tian L, Cichon J, Harnett MT, Akerboom J, Gordus A, Renninger SL, Chen TW, Bargmann CI, Orger MB, Schreiter ER, Demb JB, Gan WB, Hires SA, Looger LL (2013) An optimized fluorescent probe for visualizing glutamate neurotransmission. Nat Methods 10:162–170.

McCullumsmith RE, Sanacora G (2015) Regulation of extrasynaptic glutamate levels as a pathophysiological mechanism in disorders of motivation and addiction. Neuropsychopharmacology 40:254–255.

Miller OH, Bruns A, Ammar IB, Mueggler T, Hall BJ (2017) Synaptic Regulation of a Thalamocortical Circuit Controls Depression-Related Behavior. Cell Rep 20:1867–1880.

Miller OH, Yang L, Wang C-C, Hargroder EA, Zhang Y, Delpire E, Hall BJ (2014) GluN2B-containing NMDA receptors regulate depression-like behavior and are critical for the rapid antidepressant actions of ketamine Westbrook GL, ed. eLife 3:e03581.

Milnerwood AJ, Gladding CM, Pouladi MA, Kaufman AM, Hines RM, Boyd JD, Ko RWY, Vasuta OC, Graham RK, Hayden MR, Murphy TH, Raymond LA (2010) Early Increase in Extrasynaptic NMDA Receptor Signaling and Expression Contributes to Phenotype Onset in Huntington's Disease Mice. Neuron 65:178–190.

Minge D, Domingos C, Unichenko P, Behringer C, Pauletti A, Anders S, Herde MK, Delekate A, Gulakova P, Schoch S, Petzold GC, Henneberger C (2021) Heterogeneity and Development of Fine Astrocyte Morphology Captured by Diffraction-Limited Microscopy. Front Cell Neurosci 15 Available at: https://www.frontiersin.org/articles/10.3389/fncel.2021.669280.

Mishra A, Reynolds JP, Chen Y, Gourine AV, Rusakov DA, Attwell D (2016) Astrocytes mediate neurovascular signaling to capillary pericytes but not to arterioles. Nat Neurosci 19:1619–1627.

Moberg S, Takahashi N (2022) Neocortical layer 5 subclasses: From cellular properties to roles in behavior. Front Synaptic Neurosci 14 Available at: https://www.frontiersin.org/articles/10.3389/fnsyn.2022.1006773.

Moret C, Briley M (2011) The importance of norepinephrine in depression. Neuropsychiatr Dis Treat 7:9–13.

Mu Y, Bennett DV, Rubinov M, Narayan S, Yang C-T, Tanimoto M, Mensh BD, Looger LL, Ahrens MB (2019) Glia Accumulate Evidence that Actions Are Futile and Suppress Unsuccessful Behavior. Cell 178:27-43.e19.

Müller FE, Schade SK, Cherkas V, Stopper L, Breithausen B, Minge D, Varbanov H, Wahl-Schott C, Antoniuk S, Domingos C, Compan V, Kirchhoff F, Henneberger C, Ponimaskin E, Zeug A (2021) Serotonin receptor 4 regulates hippocampal astrocyte morphology and function. Glia 69:872–889.

Nagamine T (2020) Role of Norepinephrine in Schizophrenia: An Old Theory Applied to a New Case in Emergency Medicine. Innov Clin Neurosci 17:8–9.

Navarrete M, Perea G, Fernandez de SD, Gomez-Gonzalo M, Nunez A, Martin ED, Araque A (2012) Astrocytes mediate in vivo cholinergic-induced synaptic plasticity. PLoS Biol 10:e1001259.

Neusch C, Papadopoulos N, Muller M, Maletzki I, Winter SM, Hirrlinger J, Handschuh M, Bahr M, Richter DW, Kirchhoff F, Hulsmann S (2006) Lack of the Kir4.1 channel subunit abolishes K^+ buffering properties of astrocytes in the ventral respiratory group: impact on extracellular K^+ regulation. J Neurophysiol 95:1843–1852.

Newman EA (1999) Sodium-bicarbonate cotransport in retinal astrocytes and Müller cells of the rat. Glia 26:302–308.

Newman EA (2002) Modulation of neuronal activity by glial cells in the retina. In: The tripartite synapse. Glia in synaptic transmission, 1st ed. (Volterra A, Magistretti PJ, Haydon PG, eds), pp 199–211. New York: Oxford University Press.

Newman EA, Frambach DA, Odette LL (1984) Control of extracellular potassium levels by retinal glial cell K^+ siphoning. Science 225:1174–1175.

Nicholson C, Kamali-Zare P, Tao L (2011) Brain Extracellular Space as a Diffusion Barrier. Comput Vis Sci 14:309–325.

Nicholson C, Phillips JM (1981) Ion diffusion modified by tortuosity and volume fraction in the extracellular microenvironment of the rat cerebellum. J Physiol 321:225–257.

Nie H, Weng H-R (2009) Glutamate Transporters Prevent Excessive Activation of NMDA Receptors and Extrasynaptic Glutamate Spillover in the Spinal Dorsal Horn. J Neurophysiol 101:2041–2051.

Nortley R, Attwell D (2017) Control of brain energy supply by astrocytes. Curr Opin Neurobiol 47:80–85.

Nuriya M, Morita A, Shinotsuka T, Yamada T, Yasui M (2018) Norepinephrine induces rapid and long-lasting phosphorylation and redistribution of connexin 43 in cortical astrocytes. Biochem Biophys Res Commun 504:690–697.

Oberheim NA, Wang X, Goldman S, Nedergaard M (2006) Astrocytic complexity distinguishes the human brain. Trends Neurosci 29:547–553.

O'Donnell J, Zeppenfeld D, McConnell E, Pena S, Nedergaard M (2012) Norepinephrine: A Neuromodulator That Boosts the Function of Multiple Cell Types to Optimize CNS Performance. Neurochem Res 37:2496–2512.

Oliet SH, Piet R, Poulain DA, Theodosis DT (2004) Glial modulation of synaptic transmission: Insights from the supraoptic nucleus of the hypothalamus. Glia 47:258–267.

Oliet SHR, Piet R, Poulain DA (2001) Control of glutamate clearance and synaptic efficacy by glial coverage of neurons. Science 292:923–926.

PA Rosenberg, R Knowles, KP Knowles, Y Li (1994) Beta-adrenergic receptor-mediated regulation of extracellular adenosine in cerebral cortex in culture. J Neurosci 14:2953.

Pallas-Bazarra N, Draffin J, Cuadros R, Antonio Esteban J, Avila J (2019) Tau is required for the function of extrasynaptic NMDA receptors. Sci Rep 9:9116.

Panatier A, Theodosis DT, Mothet JP, Touquet B, Pollegioni L, Poulain DA, Oliet SH (2006) Glia-derived D-serine controls NMDA receptor activity and synaptic memory. Cell 125:775–784.

Pankratov Y, Lalo U (2015) Role for astroglial α1-adrenoreceptors in gliotransmission and control of synaptic plasticity in the neocortex. Front Cell Neurosci 9 Available at: https://www.frontiersin.org/articles/10.3389/fncel.2015.00230.

Papouin T, Ladepeche L, Ruel J, Sacchi S, Labasque M, Hanini M, Groc L, Pollegioni L, Mothet JP, Oliet SH (2012) Synaptic and extrasynaptic NMDA receptors are gated by different endogenous coagonists. Cell 150:633–646.

Parsons MP, Raymond LA (2014) Extrasynaptic NMDA Receptor Involvement in Central Nervous System Disorders. Neuron 82:279–293.

Parsons MP, Vanni MP, Woodard CL, Kang R, Murphy TH, Raymond LA (2016) Real-time imaging of glutamate clearance reveals normal striatal uptake in Huntington disease mouse models. Nat Commun 7:11251.

Paukert M, Agarwal A, Cha J, Doze VA, Kang JU, Bergles DE (2014) Norepinephrine Controls Astroglial Responsiveness to Local Circuit Activity. Neuron 82:1263–1270.

Perez-Alvarez A, Navarrete M, Covelo A, Martin ED, Araque A (2014) Structural and functional plasticity of astrocyte processes and dendritic spine interactions. J Neurosci 34:12738–12744.

Piet R, Vargova L, Sykova E, Poulain DA, Oliet SH (2004) Physiological contribution of the astrocytic environment of neurons to intersynaptic crosstalk. Proc Natl Acad Sci U A 101:2151–2155.

Poopalasundaram S, Knott C, Shamotienko OG, Foran PG, Dolly JO, Ghiani CA, Gallo V, Wilkin GP (2000) Glial heterogeneity in expression of the inwardly rectifying K^+ channel, Kir4.1, in adult rat CNS. Glia 30:362–372.

Popov A, Denisov P, Bychkov M, Brazhe A, Lyukmanova E, Shenkarev Z, Lazareva N, Verkhratsky A, Semyanov A (2020) Caloric restriction triggers morphofunctional remodeling of astrocytes and enhances synaptic plasticity in the mouse hippocampus. Cell Death Dis 11:1–17.

Potapenko ES, Biancardi VC, Zhou Y, Stern JE (2013) Astrocytes modulate a postsynaptic NMDA-$GABA_A$-receptor crosstalk in hypothalamic neurosecretory neurons. J Neurosci 33:631–640.

Pousinha PA, Mouska X, Raymond EF, Gwizdek C, Dhib G, Poupon G, Zaragosi L-E, Giudici C, Bethus I, Pacary E, Willem M, Marie H (2017) Physiological and pathophysiological control of synaptic GluN2B-NMDA receptors by the C-terminal domain of amyloid precursor protein Slutsky I, ed. eLife 6:e25659.

Rajkowska G, Stockmeier CA (2013) ASTROCYTE PATHOLOGY IN MAJOR DEPRESSIVE DISORDER: INSIGHTS FROM HUMAN POSTMORTEM BRAIN TISSUE. Curr Drug Targets 14:1225–1236.

Rauen T, Rothstein JD, Wassle H (1996) Differential expression of three glutamate transporter subtypes. Cell Tissue Res 286:325–336.

Renault-Mihara F, Mukaino M, Shinozaki M, Kumamaru H, Kawase S, Baudoux M, Ishibashi T, Kawabata S, Nishiyama Y, Sugai K, Yasutake K, Okada S, Nakamura M, Okano H (2017) Regulation of RhoA by STAT3 coordinates glial scar formation. J Cell Biol 216:2533–2550.

Romanos J, Benke D, Saab AS, Zeilhofer HU, Santello M (2019) Differences in glutamate uptake between cortical regions impact neuronal NMDA receptor activation. Commun Biol 2:127.

Rose CR, Felix L, Zeug A, Dietrich D, Reiner A, Henneberger C (2018) Astroglial Glutamate Signaling and Uptake in the Hippocampus. Front Mol Neurosci 10:451.

Rose CR, Ransom BR (1997) Gap junctions equalize intracellular Na^+ concentration in astrocytes. Glia 20:299–307.

Rothman SM, Olney JW (1987) Excitotoxicity and the NMDA receptor. Trends Neurosci 10:299–302.

Rothstein JD, Dykes-Hoberg M, Pardo CA, Bristol LA, Jin L, Kuncl RW, Kanai Y, Hediger MA, Wang Y, Schielke JP, Welty DF (1996) Knockout of glutamate transporters reveals a major role for astroglial transport in excitotoxicity and clearance of glutamate. Neuron 16:675–686.

Ruhé HG, Mason NS, Schene AH (2007) Mood is indirectly related to serotonin, norepinephrine and dopamine levels in humans: a meta-analysis of monoamine depletion studies. Mol Psychiatry 12:331–359.

Rusakov DA (2001) The role of perisynaptic glial sheaths in glutamate spillover and extracellular Ca(2+) depletion. Biophys J 81:1947–1959.

Salm AK, McCarthy KD (1989) Expression of beta-adrenergic receptors by astrocytes isolated from adult rat cortex. Glia 2:346–352.

Salm AK, McCarthy KD (1990) Norepinephrine-evoked calcium transients in cultured cerebral type 1 astroglia. Glia 3:529–538.

Santana N, Artigas F (2017) Laminar and Cellular Distribution of Monoamine Receptors in Rat Medial Prefrontal Cortex. Front Neuroanat 11:87.

Santana N, Mengod G, Artigas F (2013) Expression of α1-adrenergic receptors in rat prefrontal cortex: cellular co-localization with 5-HT2A receptors. Int J Neuropsychopharmacol 16:1139–1151.

Scheefhals N, Westra M, MacGillavry HD (2023) mGluR5 is transiently confined in perisynaptic nanodomains to shape synaptic function. Nat Commun 14:244.

Scheinin M, Lomasney JW, Hayden-Hixson DM, Schambra UB, Caron MG, Lefkowitz RJ, Fremeau RT (1994) Distribution of α2-adrenergic receptor subtype gene expression in rat brain. Mol Brain Res 21:133–149.

Schipke CG, Boucsein C, Ohlemeyer C, Kirchhoff F, Kettenmann H (2002) Astrocyte Ca^{2+} waves trigger responses in microglial cells in brain slices. FASEB J 16(2):255–257.

Schwarz LA, Luo L (2015) Organization of the Locus Coeruleus-Norepinephrine System. Curr Biol 25:R1051–R1056.

Scimemi A, Fine A, Kullmann DM, Rusakov DA (2004) NR2B-containing receptors mediate cross talk among hippocampal synapses. J Neurosci 24:4767–4777.

Sherpa AD, Xiao F, Joseph N, Aoki C, Hrabetova S (2016) Activation of beta-adrenergic receptors in rat visual cortex expands astrocytic processes and reduces extracellular space volume. Synapse 70:307–316.

Sherwood MW, Arizono M, Hisatsune C, Bannai H, Ebisui E, Sherwood JL, Panatier A, Oliet SHR, Mikoshiba K (2017) Astrocytic IP3Rs: Contribution to Ca2+ signalling and hippocampal LTP. Glia 65:502–513.

Shi X, Zhang Q, Li J, Liu X, Zhang Y, Huang M, Fang W, Xu J, Yuan T, Xiao L, Tang Y-Q, Wang X-D, Luo J, Yang W (2021) Disrupting phosphorylation of Tyr-1070 at GluN2B selectively produces resilience to depression-like behaviors. Cell Rep 36

Available at: https://www.cell.com/cell-reports/abstract/S2211-1247(21)01050-0 [Accessed April 25, 2023].

Shibasaki K, Hosoi N, Kaneko R, Tominaga M, Yamada K (2017) Glycine release from astrocytes via functional reversal of GlyT1. J Neurochem 140:395–403.

Sohal RS, Weindruch R (1996) Oxidative stress, caloric restriction, and aging. Science 273:59–63.

Somjen GG (1988) Nervenkitt: notes on the history of the concept of neuroglia. Glia 1:2–9.

Song D, Xu J, Hertz L, Peng L (2015) Regulatory volume increase in astrocytes exposed to hypertonic medium requires β1-adrenergic Na+/K+-ATPase stimulation and glycogenolysis. J Neurosci Res 93:130–139.

Srinivasan R, Huang BS, Venugopal S, Johnston AD, Chai H, Zeng H, Golshani P, Khakh BS (2015) Ca2+ signaling in astrocytes from Ip3r2−/− mice in brain slices and during startle responses in vivo. Nat Neurosci 18:708–717.

Stevens ER, Gustafson EC, Miller RF (2010) Glycine transport accounts for the differential role of glycine vs. d-serine at NMDA receptor coagonist sites in the salamander retina. Eur J Neurosci 31:808–816.

Stobart JL, Ferrari KD, Barrett MJP, Gluck C, Stobart MJ, Zuend M, Weber B (2018) Cortical Circuit Activity Evokes Rapid Astrocyte Calcium Signals on a Similar Timescale to Neurons. Neuron 98:726-735 e4.

Stogsdill JA, Ramirez J, Liu D, Kim YH, Baldwin KT, Enustun E, Ejikeme T, Ji R-R, Eroglu C (2017) Astrocytic neuroligins control astrocyte morphogenesis and synaptogenesis. Nature 551:192–197.

Subbarao KV, Hertz L (1990) Effect of adrenergic agonists on glycogenolysis in primary cultures of astrocytes. Brain Res 536:220–226.

Svoboda J, Sykova E (1991) Extracellular space volume changes in the rat spinal cord produced by nerve stimulation and peripheral injury. Brain Res 560:216–224.

Sykova E (2004) Extrasynaptic volume transmission and diffusion parameters of the extracellular space. Neuroscience 129:861–876.

Sykova E, Nicholson C (2008) Diffusion in brain extracellular space. Physiol Rev 88:1277–1340.

Szot P, Franklin A, Miguelez C, Wang Y, Vidaurrazaga I, Ugedo L, Sikkema C, Wilkinson CW, Raskind MA (2016) Depressive-like behavior observed with a minimal loss of locus coeruleus (LC) neurons following administration of 6-hydroxydopamine is associated with electrophysiological changes and reversed with precursors of norepinephrine. Neuropharmacology 101:76–86.

Takata N, Mishima T, Hisatsune C, Nagai T, Ebisui E, Mikoshiba K, Hirase H (2011) Astrocyte calcium signaling transforms cholinergic modulation to cortical plasticity in vivo. J Neurosci 31:18155–18165.

Takayasu Y, Iino M, Shimamoto K, Tanaka K, Ozawa S (2006) Glial glutamate transporters maintain one-to-one relationship at the climbing fiber-Purkinje cell synapse by preventing glutamate spillover. J Neurosci 26:6563–6572.

Tanaka K, Watase K, Manabe T, Yamada K, Watanabe M, Ichihara N, Kikuchi T, Okuyama S, Kawashima N, Hori S, Takimoto M, Wada K (1997) Epilepsy and exacerbation of brain injury in mice lacking the glutamate transporter GLT-1. Science 276:1699–1702.

Tang X-H, Zhang G-F, Xu N, Duan G-F, Jia M, Liu R, Zhou Z-Q, Yang J-J (2020) Extrasynaptic CaMKIIα is involved in the antidepressant effects of ketamine by downregulating GluN2B receptors in an LPS-induced depression model. J Neuroinflammation 17:181.

Tavares A, Handy DE, Bogdanova NN, Rosene DL, Gavras H (1996) Localization of α2A- and α2B-Adrenergic Receptor Subtypes in Brain. Hypertension 27:449–455.

Theodosis DT, Poulain DA (2001) Maternity leads to morphological synaptic plasticity in the oxytocin system. Prog Brain Res 133:49–58.

Theodosis DT, Poulain DA, Oliet SHR (2008) Activity-dependent structural and functional plasticity of astrocyte-neuron interactions. Physiol Rev 88:983–1008.

Toft-Bertelsen TL, Larsen BR, Christensen SK, Khandelia H, Waagepetersen HS, MacAulay N (2021) Clearance of activity-evoked K+ transients and associated glia cell swelling occur independently of AQP4: A study with an isoform-selective AQP4 inhibitor. Glia 69:28–41.

Torres-Platas SG, Nagy C, Wakid M, Turecki G, Mechawar N (2016) Glial fibrillary acidic protein is differentially expressed across cortical and subcortical regions in healthy brains and downregulated in the thalamus and caudate nucleus of depressed suicides. Mol Psychiatry 21:509–515.

Tran CHT, Peringod G, Gordon GR (2018) Astrocytes Integrate Behavioral State and Vascular Signals during Functional Hyperemia. Neuron 100:1133-1148 e3.

Tsai HH, Li H, Fuentealba LC, Molofsky AV, Taveira-Marques R, Zhuang H, Tenney A, Murnen AT, Fancy SPJ, Merkle F, Kessaris N, Alvarez-Buylla A, Richardson WD,

Rowitch DH (2012) Regional astrocyte allocation regulates CNS synaptogenesis and repair. Science 337:358–362.

Uno Y, Coyle JT (2019) Glutamate hypothesis in schizophrenia. Psychiatry Clin Neurosci 73:204–215.

Valtcheva S, Venance L (2016) Astrocytes gate Hebbian synaptic plasticity in the striatum. Nat Commun 7:13845.

van Aerde KI, Feldmeyer D (2015) Morphological and Physiological Characterization of Pyramidal Neuron Subtypes in Rat Medial Prefrontal Cortex. Cereb Cortex 25:788–805.

Van De Werd HJJM, Rajkowska G, Evers P, Uylings HBM (2010) Cytoarchitectonic and chemoarchitectonic characterization of the prefrontal cortical areas in the mouse. Brain Struct Funct 214:339–353.

Vardjan N, Kreft M, Zorec R (2014) Dynamics of β-adrenergic/cAMP signaling and morphological changes in cultured astrocytes. Glia 62:566–579.

Veruki ML, Zhou Y, Castilho A, Morgans CW, Hartveit E (2019) Extrasynaptic NMDA Receptors on Rod Pathway Amacrine Cells: Molecular Composition, Activation, and Signaling. J Neurosci 39:627–650.

Wahis J, Holt MG (2021) Astrocytes, Noradrenaline, α1-Adrenoreceptors, and Neuromodulation: Evidence and Unanswered Questions. Front Cell Neurosci 15:645691.

Walch E, Murphy TR, Cuvelier N, Aldoghmi M, Morozova C, Donohue J, Young G, Samant A, Garcia S, Alvarez C, Bilas A, Davila D, Binder DK, Fiacco TA (2020) Astrocyte-Selective Volume Increase in Elevated Extracellular Potassium

Conditions Is Mediated by the Na+/K+ ATPase and Occurs Independently of Aquaporin 4. ASN Neuro 12:1759091420967152.

Walz W (1987) Swelling and potassium uptake in cultured astrocytes. Can J Physiol Pharmacol 65:1051–1057.

Walz W (1988) Physiological consequences of activating serotonin receptors. In: Glial Cell Receptors (Kimelberg HK, ed), pp 121–130. New York: Raven Press.

Walz W (1992) Mechanism of rapid K^+-induced swelling of mouse astrocytes. Neurosci Lett 135:243–246.

Walz W, Mukerji S (1988) Lactate production and release in cultured astrocytes. Neurosci Lett 86:296–300.

Wang C-C, Held RG, Chang S-C, Yang L, Delpire E, Ghosh A, Hall BJ (2011) A Critical Role for GluN2B-Containing NMDA Receptors in Cortical Development and Function. Neuron 72:789–805.

Wang H, Stradtman GG, Wang X-J, Gao W-J (2008) A specialized NMDA receptor function in layer 5 recurrent microcircuitry of the adult rat prefrontal cortex. Proc Natl Acad Sci 105:16791–16796.

Wilson JX, Walz W (1988) Catecholamine uptake into cultured mouse astrocytes. In: Trace Amines (Boulton AA, ed), pp 301–305. Humana Press.

Witcher MR, Park YD, Lee ML, Sharma S, Harris KM, Kirov SA (2010) Three-dimensional relationships between perisynaptic astroglia and human hippocampal synapses. Glia 58:572–587.

Woo DH, Han KS, Shim JW, Yoon BE, Kim E, Bae JY, Oh SJ, Hwang EM, Marmorstein AD, Bae YC, Park JY, Lee CJ (2012) TREK-1 and Best1 channels mediate fast and slow glutamate release in astrocytes upon GPCR activation. Cell 151:25–40.

Wotton CA, Cross CD, Bekar LK (2020) Serotonin, norepinephrine, and acetylcholine differentially affect astrocytic potassium clearance to modulate somatosensory signaling in male mice. J Neurosci Res 98:964–977.

Wurm A, Iandiev I, Hollborn M, Wiedemann P, Reichenbach A, Zimmermann H, Bringmann A, Pannicke T (2008) Purinergic receptor activation inhibits osmotic glial cell swelling in the diabetic rat retina. Exp Eye Res 87:385–393.

Xie L, Kang H, Xu Q, Chen MJ, Liao Y, Thiyagarajan M, O'Donnell J, Christensen DJ, Nicholson C, Iliff JJ, Takano T, Deane R, Nedergaard M (2013) Sleep drives metabolite clearance from the adult brain. Science 342:373–377.

Yang Q, Zhu G, Liu D, Ju J-G, Liao Z-H, Xiao Y-X, Zhang Y, Chao N, Wang J, Li W, Luo J-H, Li S-T (2017) Extrasynaptic NMDA receptor dependent long-term potentiation of hippocampal CA1 pyramidal neurons. Sci Rep 7:3045.

Ye L, Haroon MA, Salinas A, Paukert M (2017) Comparison of GCaMP3 and GCaMP6f for studying astrocyte Ca2+ dynamics in the awake mouse brain. PLoS One 12:e0181113.

Yu X, Taylor AMW, Nagai J, Golshani P, Evans CJ, Coppola G, Khakh BS (2018) Reducing Astrocyte Calcium Signaling In Vivo Alters Striatal Microcircuits and Causes Repetitive Behavior. Neuron 99:1170-1187.e9.

Zhang H, Sulzer D (2003) Glutamate spillover in the striatum depresses dopaminergic transmission by activating group I metabotropic glutamate receptors. J Neurosci 23:10585–10592.

Zhang H, Verkman AS (2010) Microfiberoptic measurement of extracellular space volume in brain and tumor slices based on fluorescent dye partitioning. Biophys J 99:1284–1291.

Zhao J, Verwer RWH, van Wamelen DJ, Qi X-R, Gao S-F, Lucassen PJ, Swaab DF (2016) Prefrontal changes in the glutamate-glutamine cycle and neuronal/glial glutamate transporters in depression with and without suicide. J Psychiatr Res 82:8–15.

Zhou X, Ding Q, Chen Z, Yun H, Wang H (2013) Involvement of the GluN2A and GluN2B Subunits in Synaptic and Extrasynaptic N-methyl-d-aspartate Receptor Function and Neuronal Excitotoxicity *. J Biol Chem 288:24151–24159.

Zhou Z, Ikegaya Y, Koyama R (2019) The Astrocytic cAMP Pathway in Health and Disease. Int J Mol Sci 20.